Neutron and x-ray scattering studies of superconductors

B. Keimer

Max-Planck-Institute for Solid State Research

lecture 1

- **conventional superconductors**

inelastic nuclear neutron scattering from phonons

- **unconventional superconductors**

magnetic structure determination by elastic magnetic neutron scattering

inelastic magnetic neutron scattering from magnons and paramagnons

Max-Planck-Institut für Festkörperforschung

Neutron and x-ray scattering studies of superconductors

lecture 2: unconventional superconductors

- magnetic neutron scattering continued
- resonant inelastic x-ray scattering from magnons and paramagnons
- resonant elastic x-ray scattering from charge density waves

lecture 3: cuprate and nickelate superlattices

- orbital occupation
- magnetic order
- charge density waves

Max-Planck-Institut für Festkörperforschung

Neutron scattering

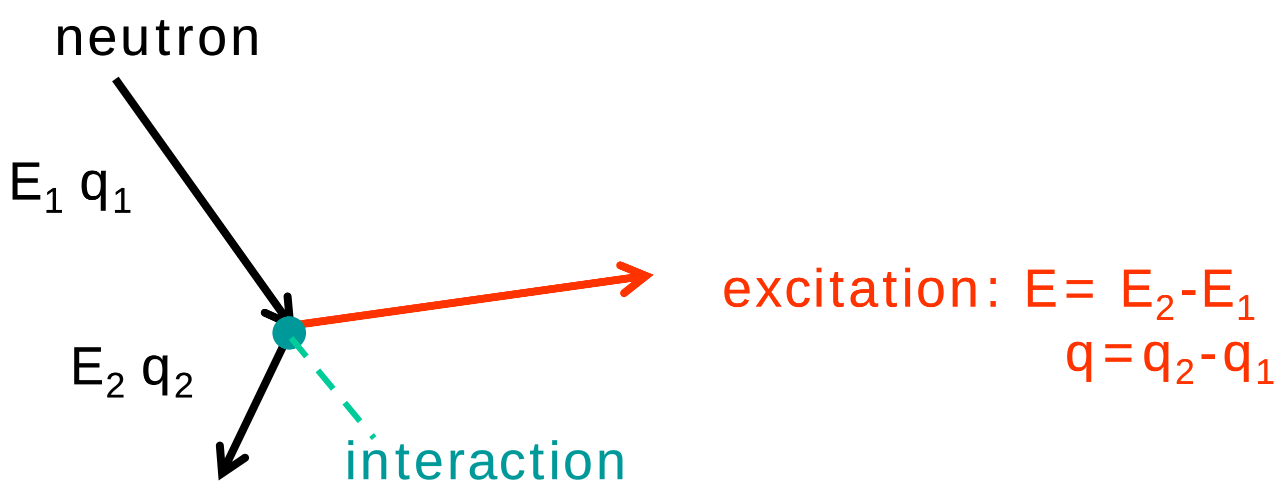

strong (nuclear) interaction

elastic	lattice structure
inelastic	lattice dynamics

magnetic (dipole-dipole) interaction

elastic	magnetic structure
inelastic	magnetic excitations

Max-Planck-Institut für Festkörperforschung

Neutron sources

research reacor

$$^{235}U + n \rightarrow A + B + 2.3n$$

FRM-II
Garching, Germany

spectrum

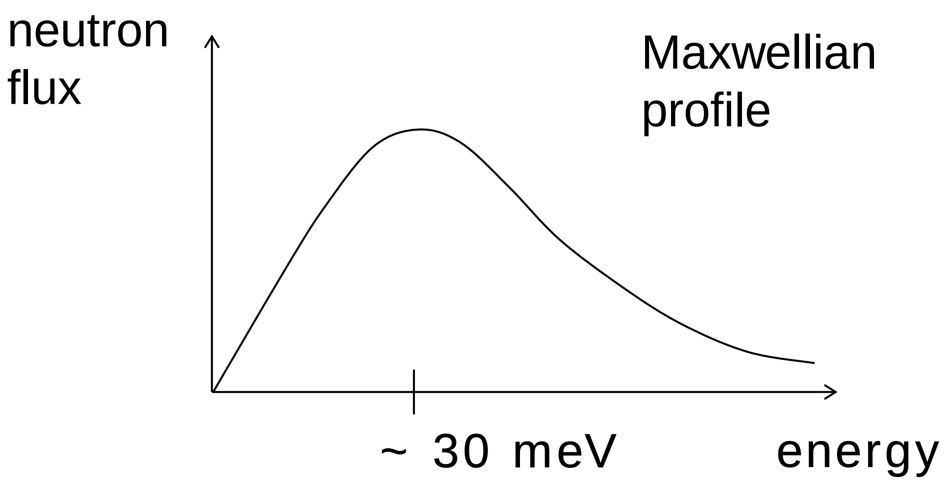

Max-Planck-Institut für Festkörperforschung

Neutron sources

spallation source

$$p + Hg \rightarrow A + B + xn$$

SNS
Oak Ridge, TN

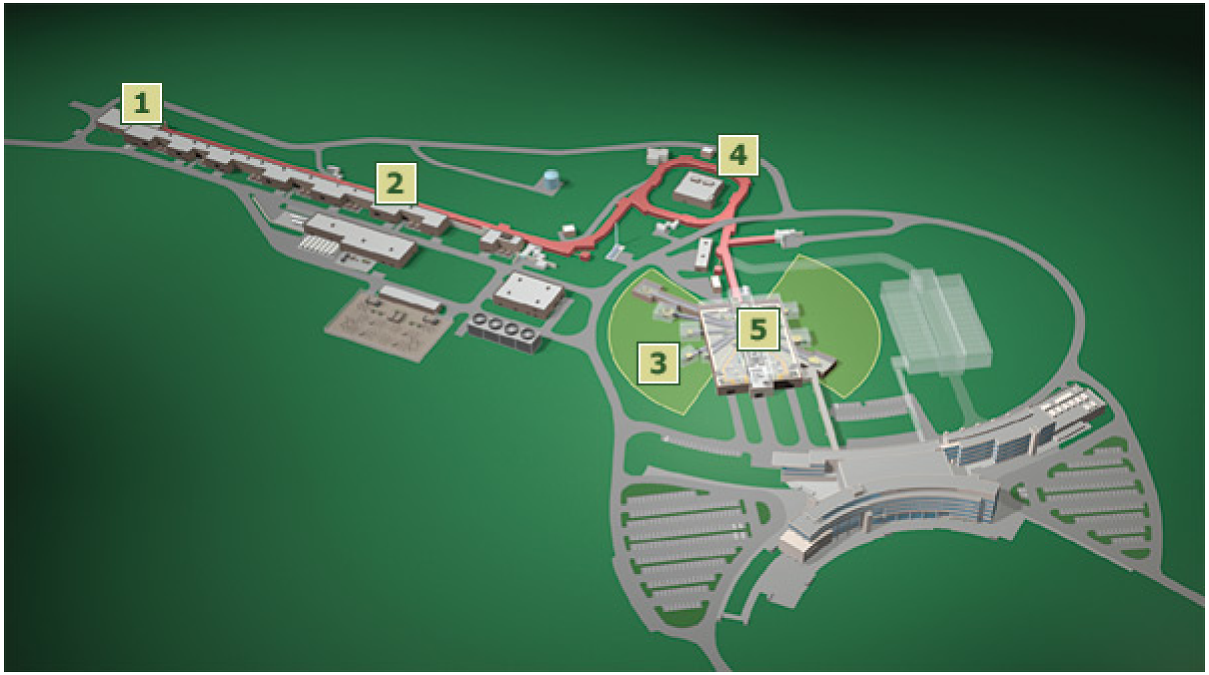

1. Source
2. Linac
3. Beamlines
4. Accumulator ring
5. Target area

Max-Planck-Institut
für Festkörperforschung

Elastic neutron scattering

basic quantity: differential cross-section $\dfrac{d\sigma}{d\Omega}$

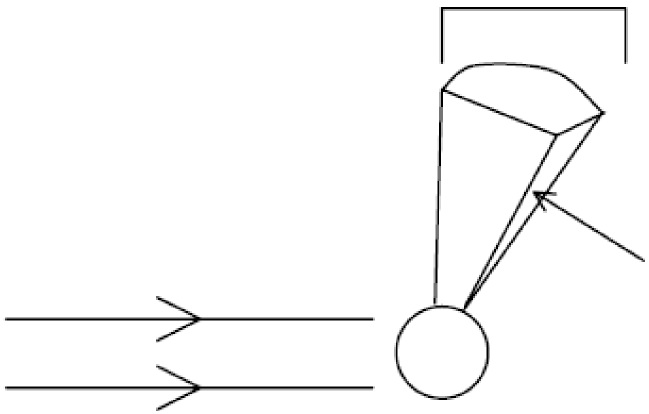

detector

$\Delta\Omega$ solid angle element covered by detector

incident neutron beam, flux $\phi = \dfrac{\text{\# of neutrons}}{\text{area} \cdot \text{time}}$

$\dfrac{d\sigma}{d\Omega}$ = # of neutrons scattered into solid angle element $d\Omega$ per unit time, normalized to incident flux.

dimensions: $\left[\dfrac{d\sigma}{d\Omega}\right] = \dfrac{1}{[\Delta\Omega]\,[t]\,[\phi]} =$ area

dimensionless

Elastic neutron scattering

calculation of $\frac{d\sigma}{d\Omega}$ through Fermi's Golden Rule:

transition rate (# of transitions per unit time): $W = \frac{2\pi}{\hbar}\left|\left\langle \vec{k}_f \right| V \left| \vec{k}_i \right\rangle\right|^2 \underbrace{\rho_f(E)}_{\text{Density of final states}}$

$$\left.\begin{aligned} |k_i\rangle &= \frac{1}{\sqrt{L^3}} e^{i\vec{k}_i\cdot\vec{r}} \\ |k_f\rangle &= \frac{1}{\sqrt{L^3}} e^{i\vec{k}_f\cdot\vec{r}} \end{aligned}\right\} \text{plane waves}$$

incident neutron flux: $\frac{\text{velocity}}{L^3} = \frac{\hbar k_i}{m_n L^3}$

$k_i = k_f$ for elastic scattering

$$\rho_f(E) = \underbrace{\left(\frac{L}{2\pi}\right)^3}_{\substack{\text{density of}\\ \text{states in}\\ k\text{-space}}} \frac{d\vec{k}_f}{dE}$$

$$d\vec{k}_f = k_f^{\,2} dk_f d\Omega$$

$$\rho_f(E) = \left(\frac{L}{2\pi}\right)^3 k_f^{\,2} \frac{dk_f}{dE} d\Omega = \left(\frac{L}{2\pi}\right)^3 \frac{m_n k_f}{\hbar^2} d\Omega \qquad \text{with} \quad \frac{dE}{dk_f} = \frac{\hbar^2 k_f}{m_n}$$

$$\Rightarrow \frac{d\sigma}{d\Omega} = \frac{W}{\text{incident flux}} = \left(\frac{m_n}{2\pi\hbar^2}\right)^2 \left|\int V e^{i(\vec{k}_i - \vec{k}_f)\cdot\vec{r}} d\vec{r}\right|^2$$

$$= \left(\frac{m_n}{2\pi\hbar^2}\right)^2 \left|\int V(\vec{r}) e^{-i\vec{Q}\cdot\vec{r}} d\vec{r}\right|^2$$

"Born approximation"

Max-Planck-Institut für Festkörperforschung

Elastic nuclear neutron scattering

For short range strong force, use approximate interaction potential

$$V(\vec{r}) = \frac{2\pi\hbar^2}{m_n} b\ \delta(\vec{r} - \vec{R})$$

"scattering length"

position of nucleus

scattering length b ~ size of nucleus ~ 10^{-15} m

for single nucleus: $\frac{d\sigma}{d\Omega} = |b|^2$

total cross section: $\sigma = \int \frac{d\sigma}{d\Omega} d\Omega = 4\pi b^2$

lattice of nuclei: $V(\vec{r}) = \frac{2\pi\hbar^2}{m_n} \sum_{\vec{R}} b_{\vec{R}}\ \delta(\vec{r} - \vec{R})$

$b_{\vec{R}}$: scattering length of nucleus at lattice site $\vec{R}$

$$\frac{d\sigma}{d\Omega} = \left| \int d\vec{r} \sum_{R} b_R\ \delta(\vec{r} - \vec{R}) e^{i\vec{Q}\cdot\vec{r}} \right|^2 = \left| \sum_{R} b_R\ e^{i\vec{Q}\cdot\vec{R}} \right|^2 = b^2 \frac{N(2\pi)^3}{v_o} \sum_{\vec{K}} \delta(\vec{Q} - \vec{K})$$

Bragg peaks
at reciprocal lattice vectors K

for unit cell with several atoms, basis vector $\vec{d}$

$$\frac{d\sigma}{d\Omega} = N \frac{(2\pi)^3}{v_0} \sum_{\vec{K}} \delta(\vec{Q} - \vec{K}) \left| F_N(\vec{K}) \right|^2$$

$$F_N(\vec{K}) = \sum_{\vec{d}} e^{i\vec{Q}\cdot\vec{d}} b_{\vec{d}}$$

"nuclear structure factor"

Neutron scattering lengths

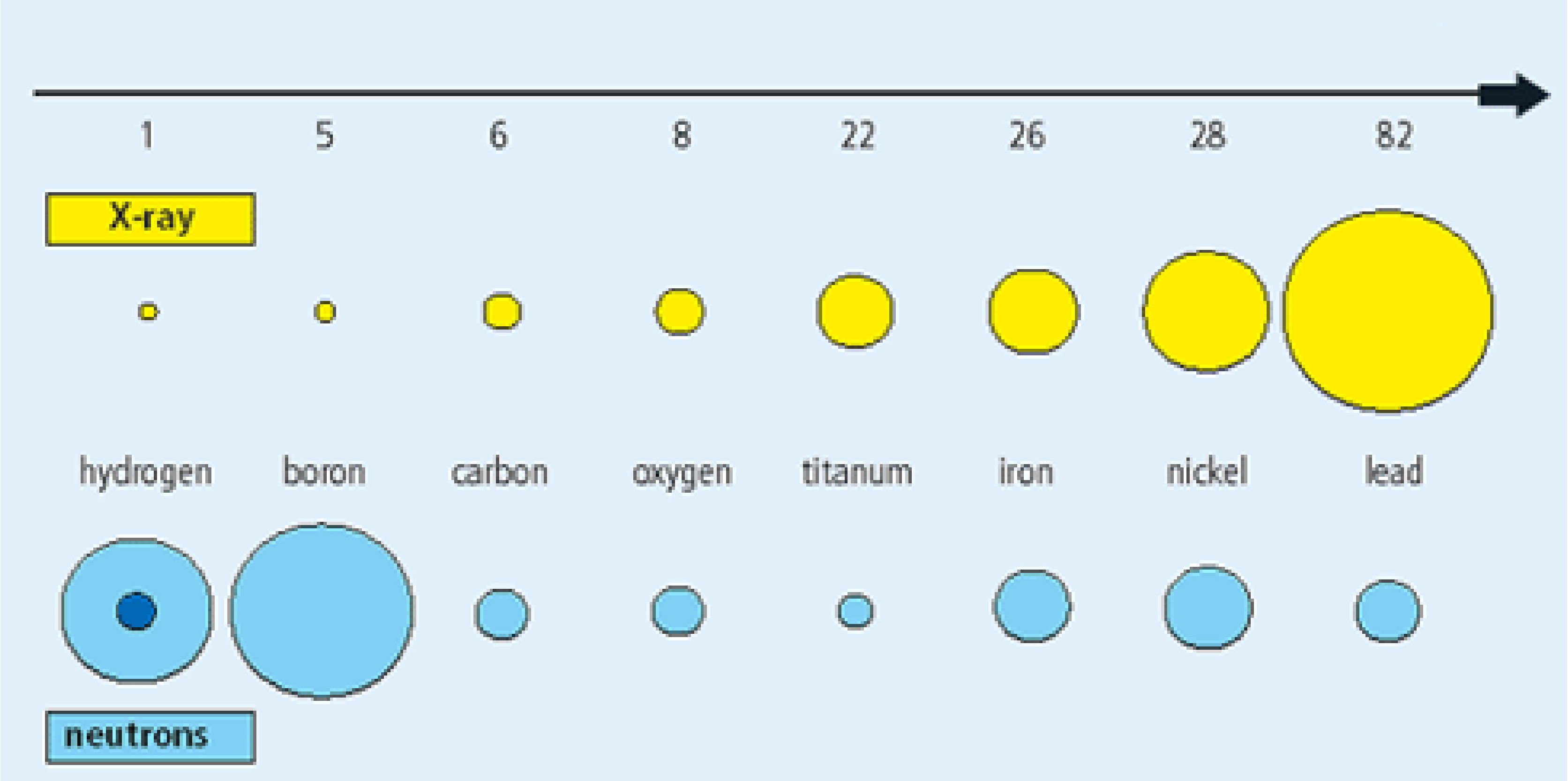

Neutron radiography

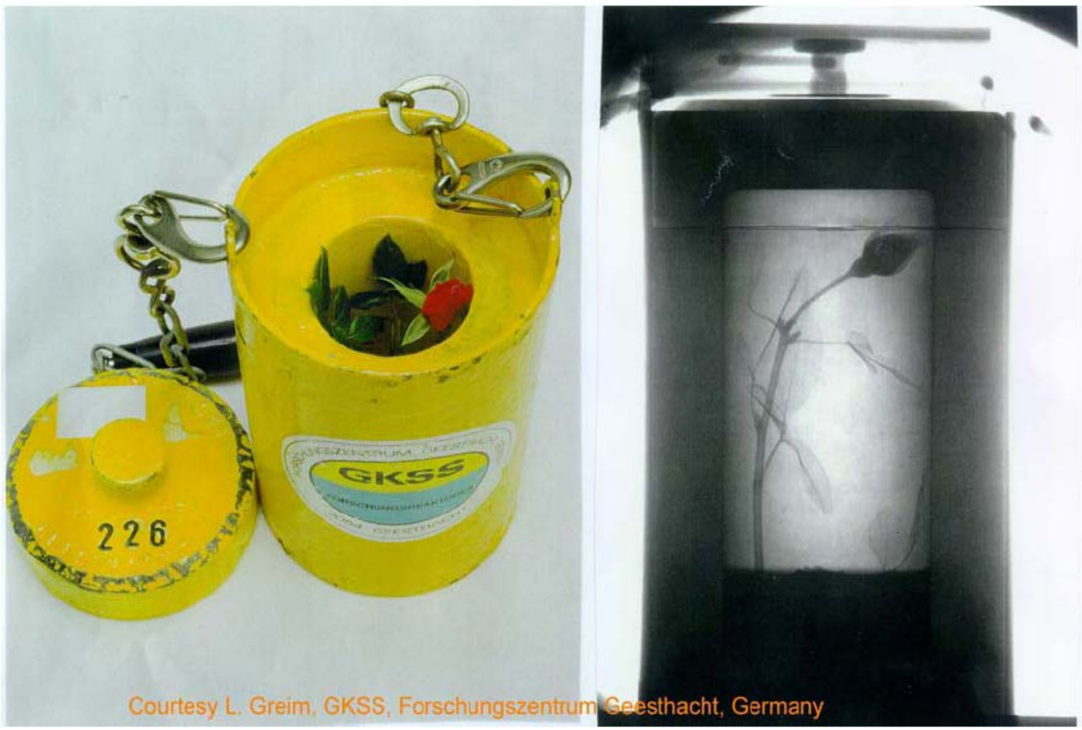

Courtesy L. Greim, GKSS, Forschungszentrum Geesthacht, Germany

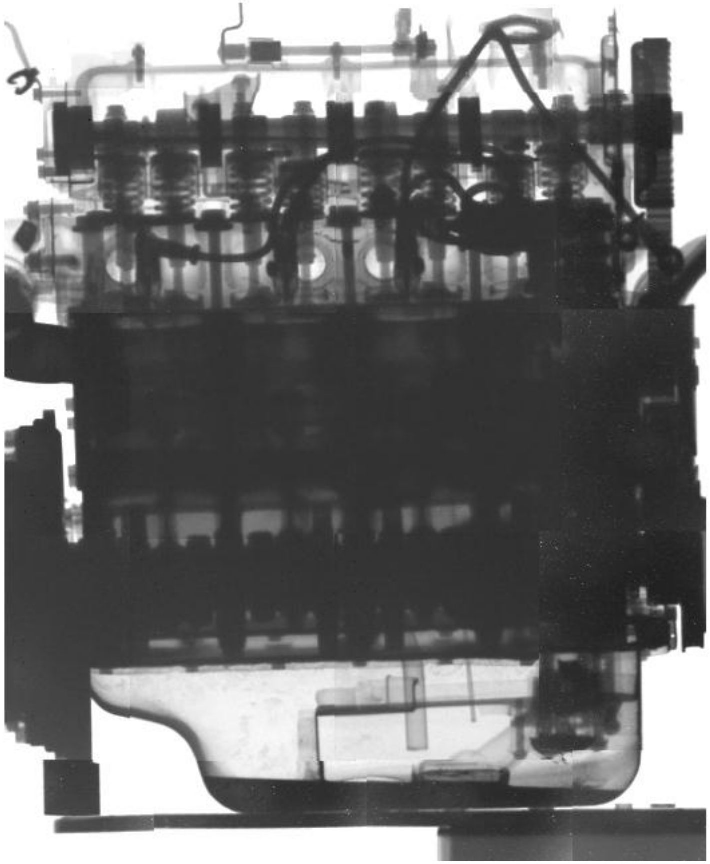

für Festkörperforschung

Inelastic neutron scattering

elastic cross section $$\frac{d\sigma}{d\Omega} = \frac{\text{\# of neutrons scattered into } d\Omega}{(\text{unit time}) \bullet (\text{incident flux})}$$

inelastic cross section $$\frac{d^2\sigma}{dE d\Omega} = \frac{\text{\# of neutrons scattered into } d\Omega}{(\text{unit time}) \bullet (\text{incident flux}) \bullet (\text{energy})}$$

inelastic nuclear neutron scattering

$$\frac{d^2\sigma}{d\Omega\, dE} = \frac{k_f}{k_i} \frac{1}{2\pi\hbar} \sum_{jj'} b_{j'} b_j \int_{-\infty}^{\infty} \sum_{\lambda_i} p_{\lambda_i} \left\langle \lambda_i \left| e^{-i\mathbf{QR}_{j'}(0)} e^{i\mathbf{QR}_j(t)} \right| \lambda_i \right\rangle e^{-i\omega t} dt$$

$|\lambda_i\rangle$ $|\lambda_f\rangle$ initial, final state of sample

$$\hbar\omega = \frac{\hbar^2 k_i^2}{2m_n} - \frac{\hbar^2 k_f^2}{2m_n} = E_{\lambda_i} - E_{\lambda_f}$$ energy of excitation created by neutron in sample

$p_{\lambda_i} = \exp(-E_{\lambda_i}\beta)/Z \quad Z = \sum_{\lambda_i} \exp(-E_{\lambda_i}\beta)$ partition function

Inelastic nuclear neutron scattering

$$\frac{d^2\sigma}{d\Omega\, dE} = \frac{k_f}{k_i}\frac{1}{2\pi\hbar}\frac{\sigma_{coh}}{4\pi}\sum_{jj'}\int_{-\infty}^{\infty}\left\langle e^{-i\mathbf{Q}\mathbf{R}_{j'}(0)} e^{i\mathbf{Q}\mathbf{R}_j(t)}\right\rangle \exp(-i\omega t)\, dt$$

$\langle e^{\cdots} e^{\cdots}\rangle = \sum p_{\lambda_i} \langle\lambda_i| e^{\cdots} e^{\cdots} |\lambda_i\rangle$ thermal average $\sigma_{coh} = 4\pi(\overline{b})^2$

$|\lambda\rangle$ characterized by population n_s of phonons of energy $\hbar\omega_s(\vec{k})$ in branch s

Debye-Waller factor due to thermal lattice vibrations

$$\frac{d^2\sigma}{d\Omega\, dE} = \frac{\sigma_{coh}}{4\pi}\frac{k_f}{k_i}\frac{(2\pi)^3}{v_0}\frac{1}{2M} e^{-2W} \sum_s \sum_\eta \frac{(\mathbf{Q}\cdot\mathbf{e}_s)^2}{\omega_s} \times$$

$$\{\langle n_s + 1\rangle\, \delta(\omega - \omega_s)\, \delta(\mathbf{Q} - \mathrm{q} - \mathbf{K}) + \langle n_s\rangle\, \delta(\omega + \omega_s)\, \delta(\mathbf{Q} + \mathrm{q} - \mathbf{K})\}$$

phonon creation
neutron energy loss

phonon annihilaion
neutron energy gain

für Festkörperforschung

Triple-axis spectrometer

$$\hbar\omega = \frac{\hbar^2}{2m}(k_f^{\ 2} - k_i^{\ 2})$$

$$q = k_f - k_i$$

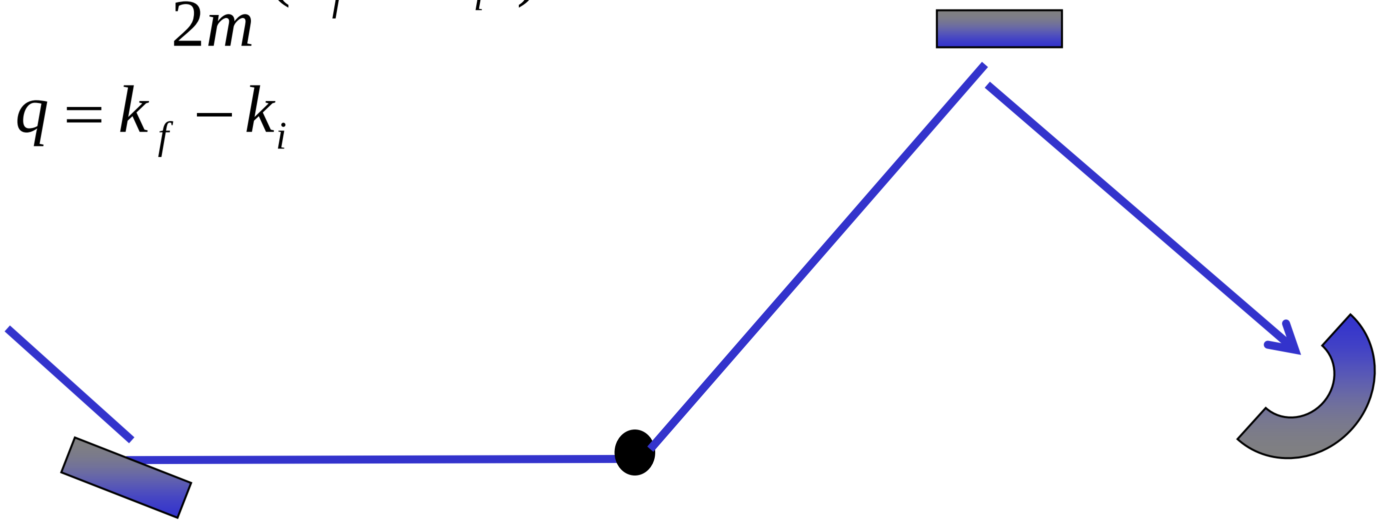

Max-Planck-Institut für Festkörperforschung

Phonon dispersions in Pb

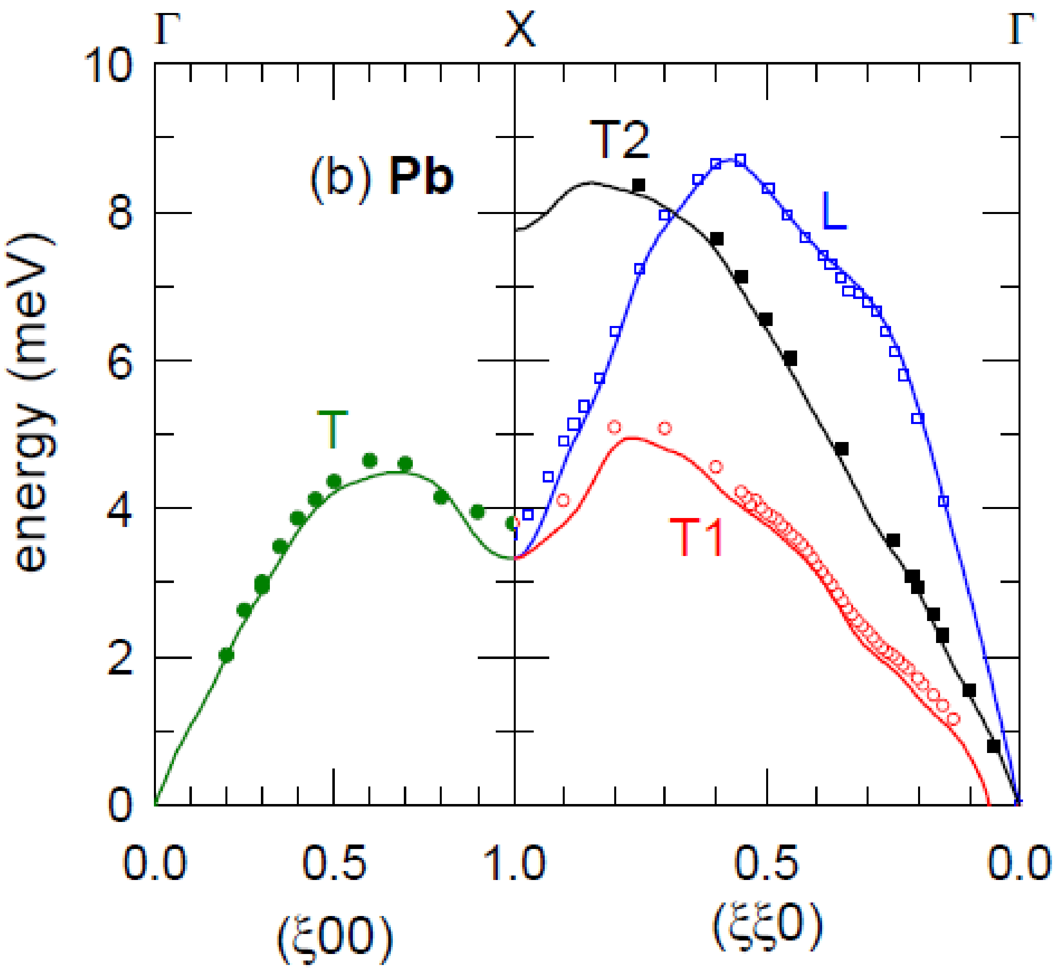

excellent agreement with ab-initio lattice dynamics

Munnikes, Boeri et al.

für Festkörperforschung

Electron-phonon interaction

electron-phonon interaction in simple metals predicted by ab-initio LDA

example MgB_2

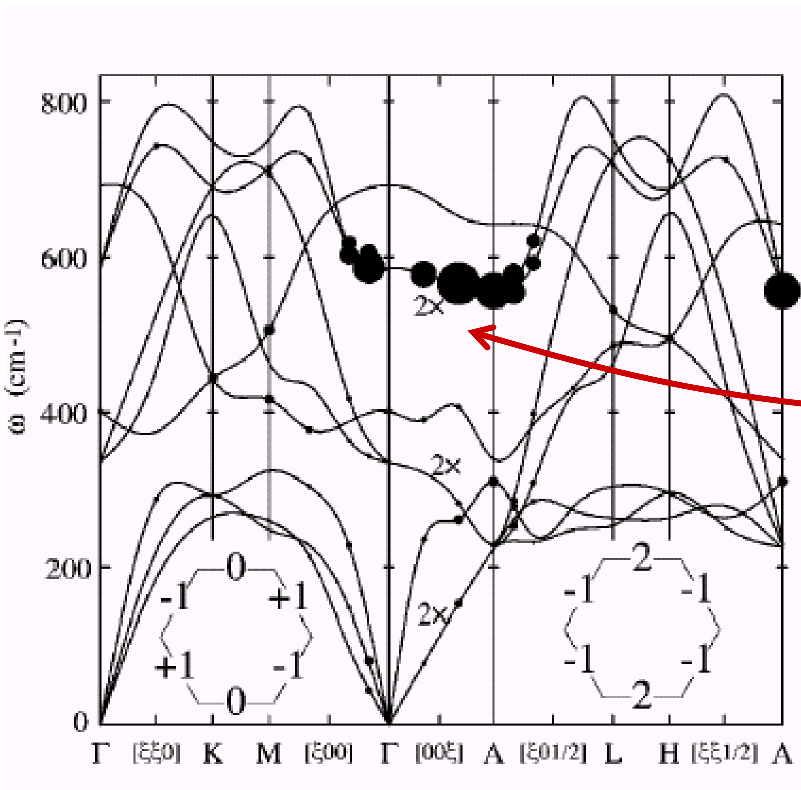

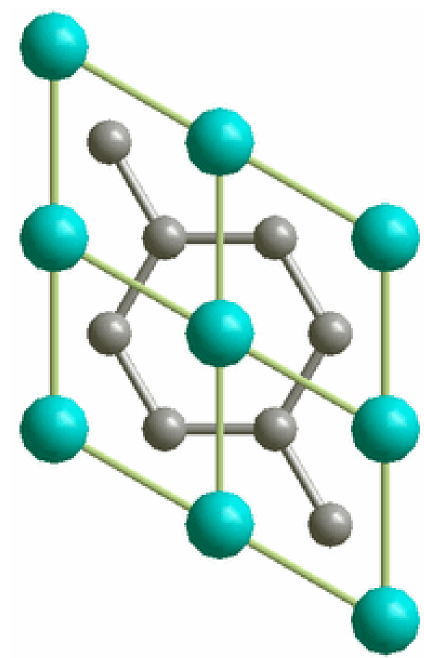

strong coupling
short phonon lifetime

Kong et al., PRB 2001

typical phonon linewidth: 1-100 µeV

Conventional superconductors

understanding based on **quasiparticles**

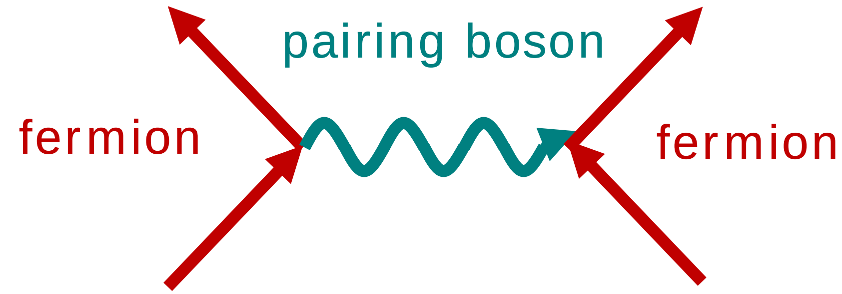

fermionic spectrum from tunneling

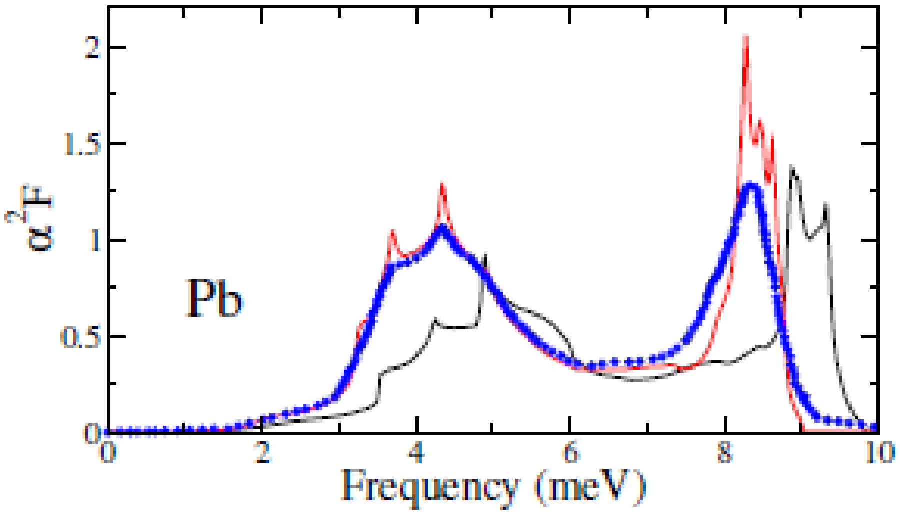

experimental tunnel spectrum

calculated spectrum based on phonon dispersions from neutrons

Resonant mode in conventional superconductors

phonon dispersion

T > T_c **T < T_c**

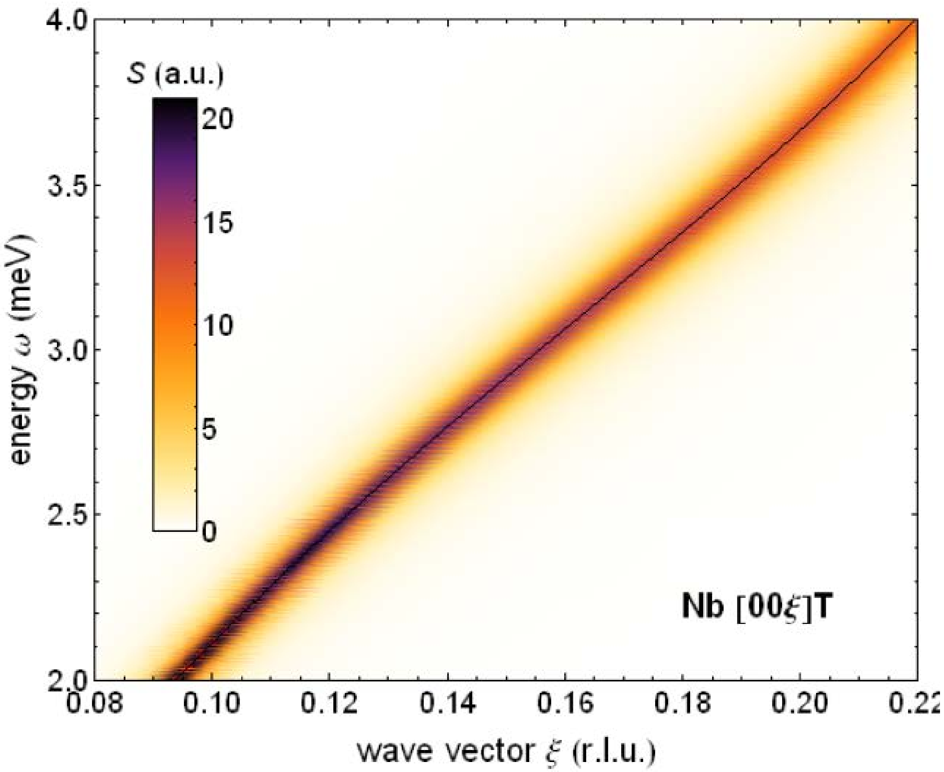

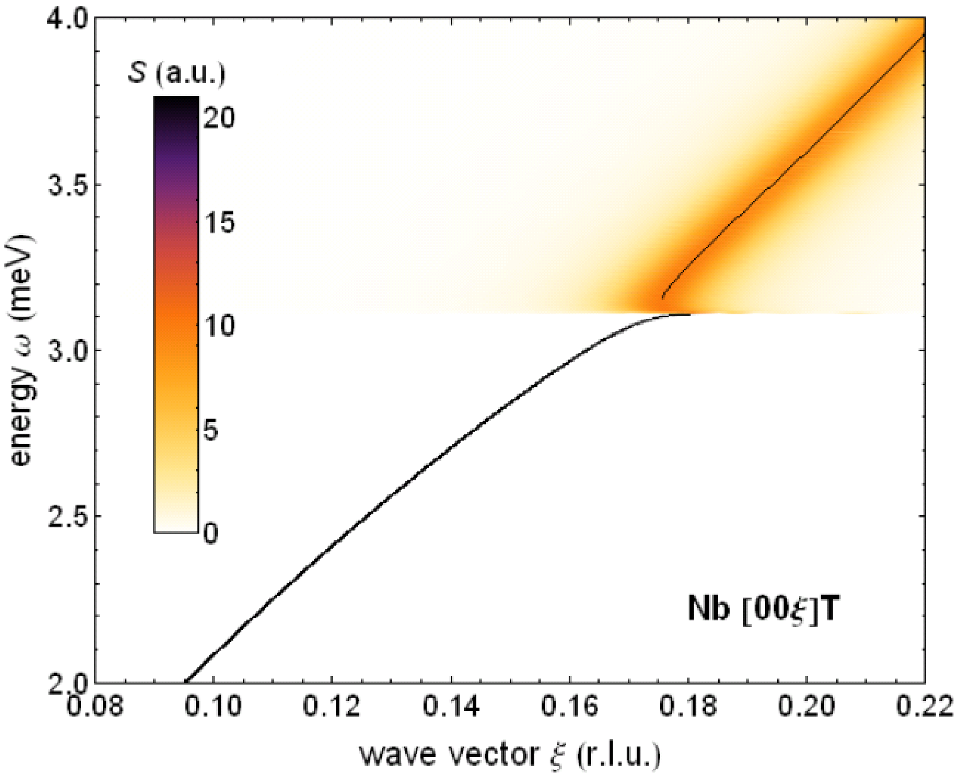

N. Munnikes after Allen et al., PRB 1997

feedback of pairing interaction on intermediate boson

Resonant mode in conventional superconductors

first observed in borocarbides

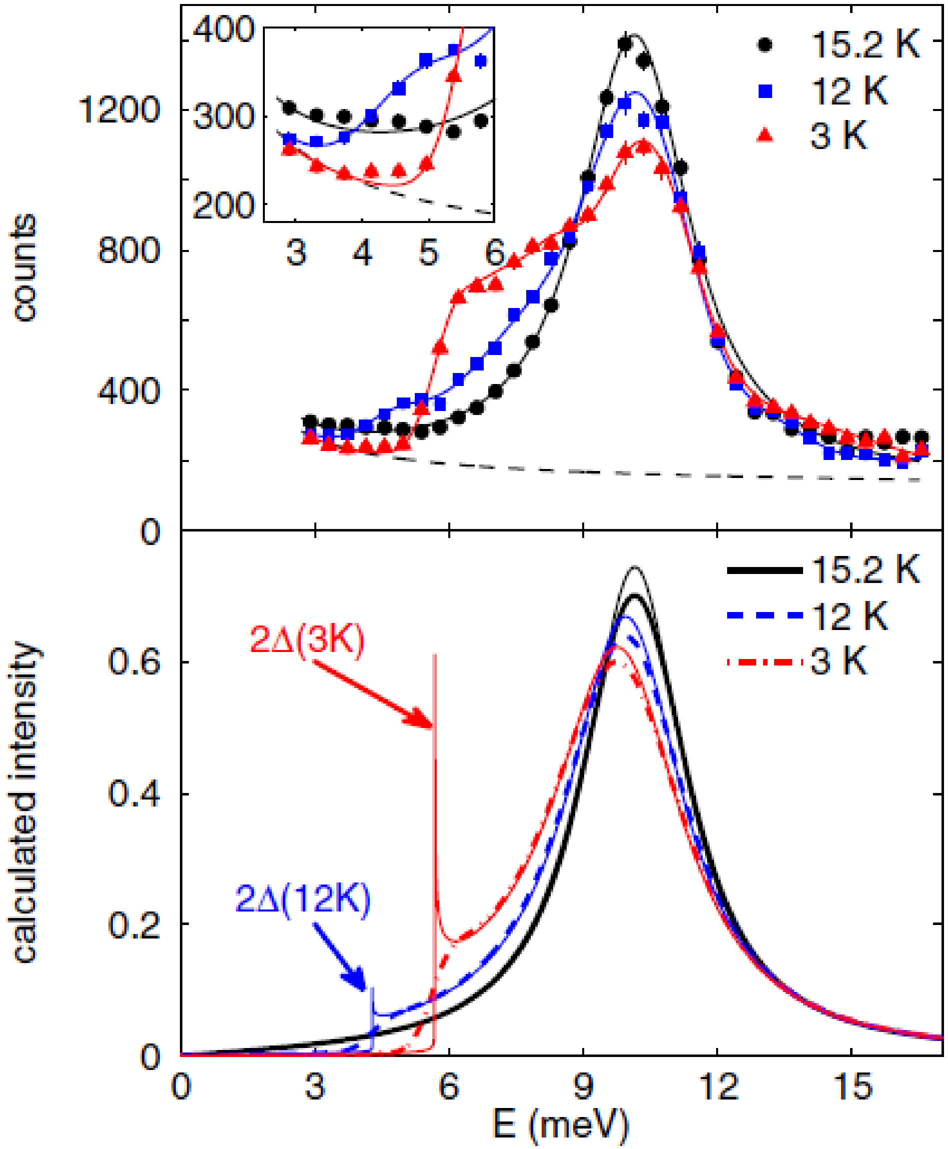

Stassis et al., PRB 1997
Weber et al., PRL 2008

Neutron spin echo spectroscopy

$$\hbar\omega = \frac{\hbar^2}{2m}(k_f^{\ 2} - k_i^{\ 2})$$

$$q = k_f - k_i$$

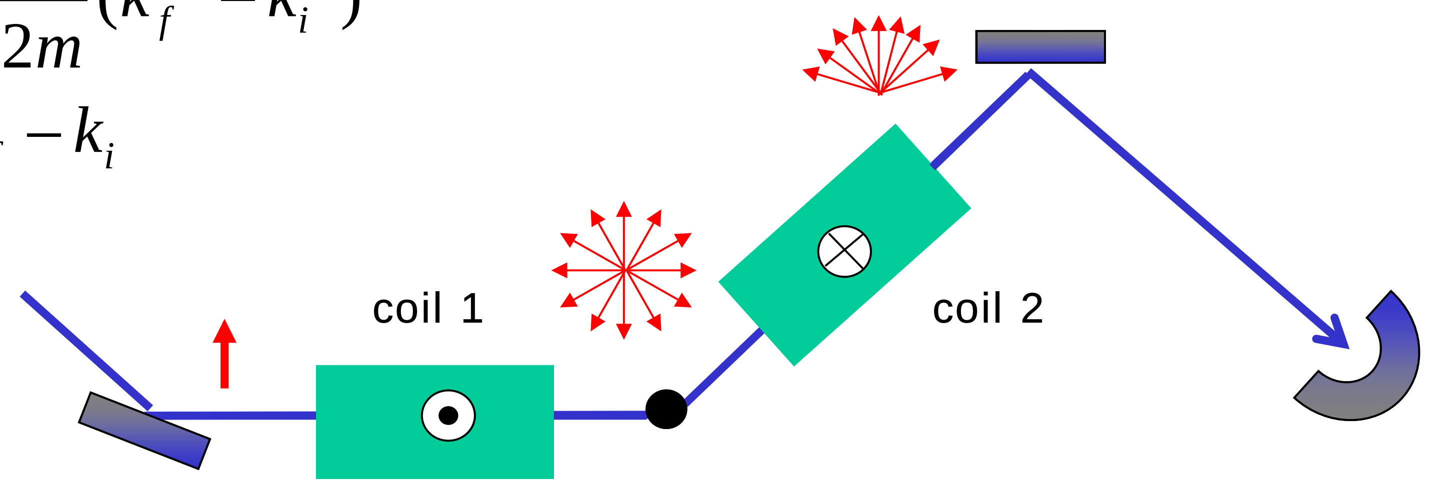

triple axis spectrometer: excitation energy ~ 1-100 meV
energy resolution ~ 0.1-10 meV

triple axis – spin echo spectrometer: excitation energy ~ 1-100 meV
energy resolution ~ 1 – 100 μeV

3 orders of magnitude gain in energy resolution
→ possible to resolve excitation lifetimes in solids

für Festkörperforschung

TRISP Spectrometer at FRM-II

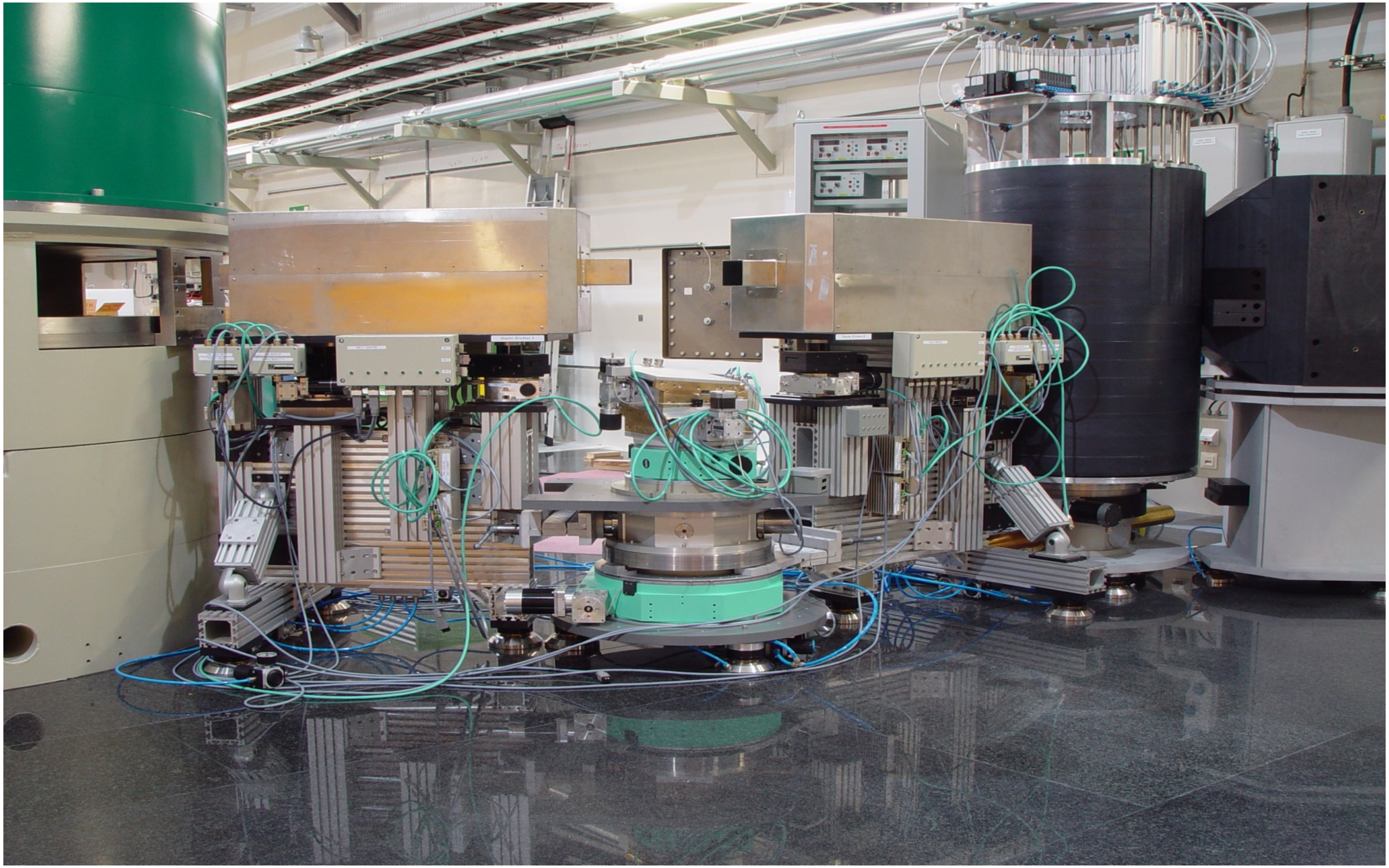

Electrn-phonon interaction

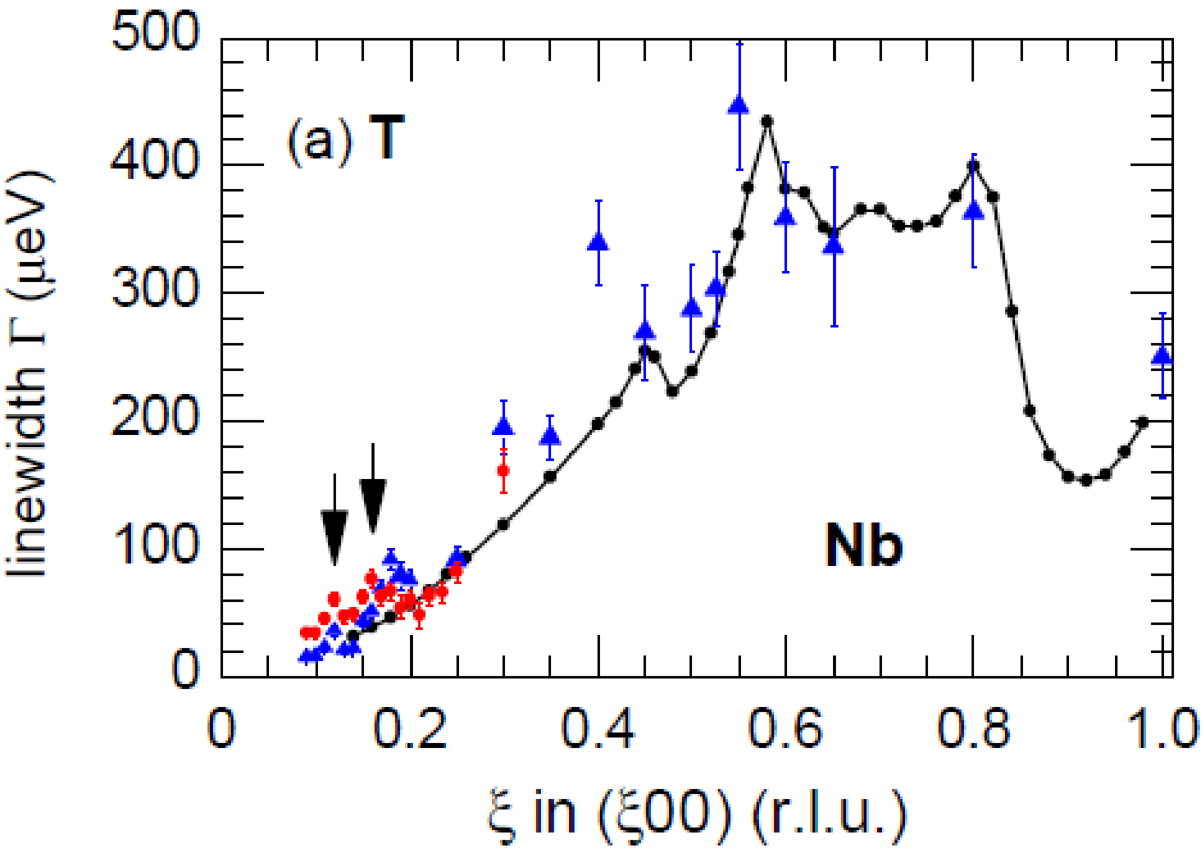

electron-phonon linewidths in good agreement with ab-initio lattice dynamics

Munnikes, Boeri et al.

Electron-phonon interaction in Pb

lifetime renormalization below superconducting T_c = 7.2 K

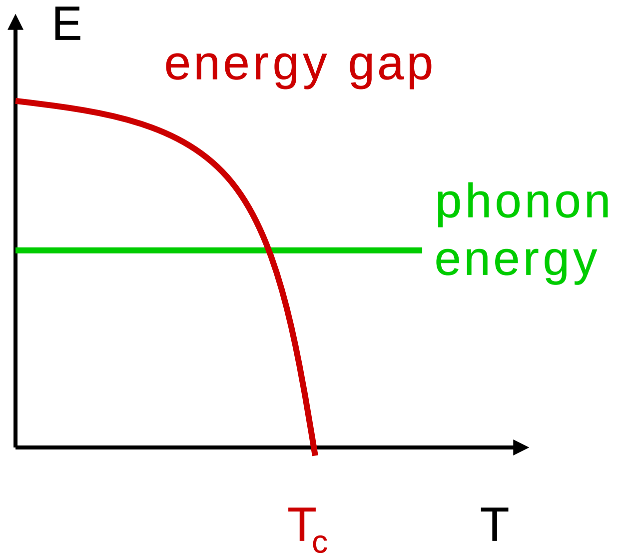

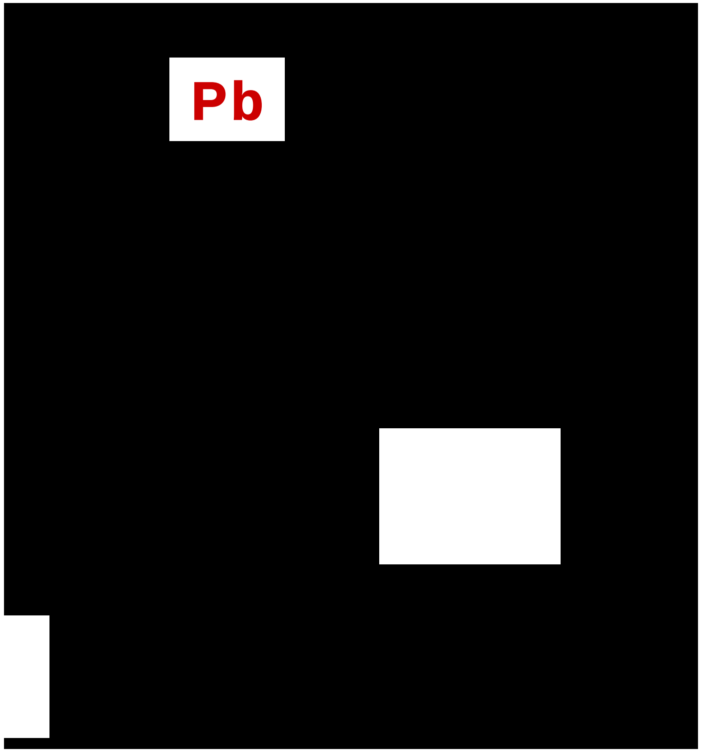

Keller et al., PRL 2006

Electron-phonon interaction in Pb

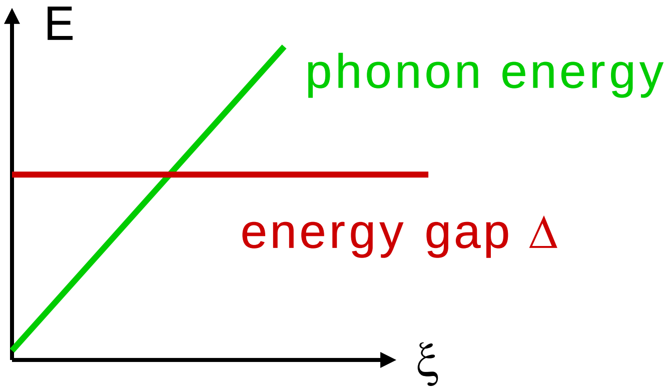

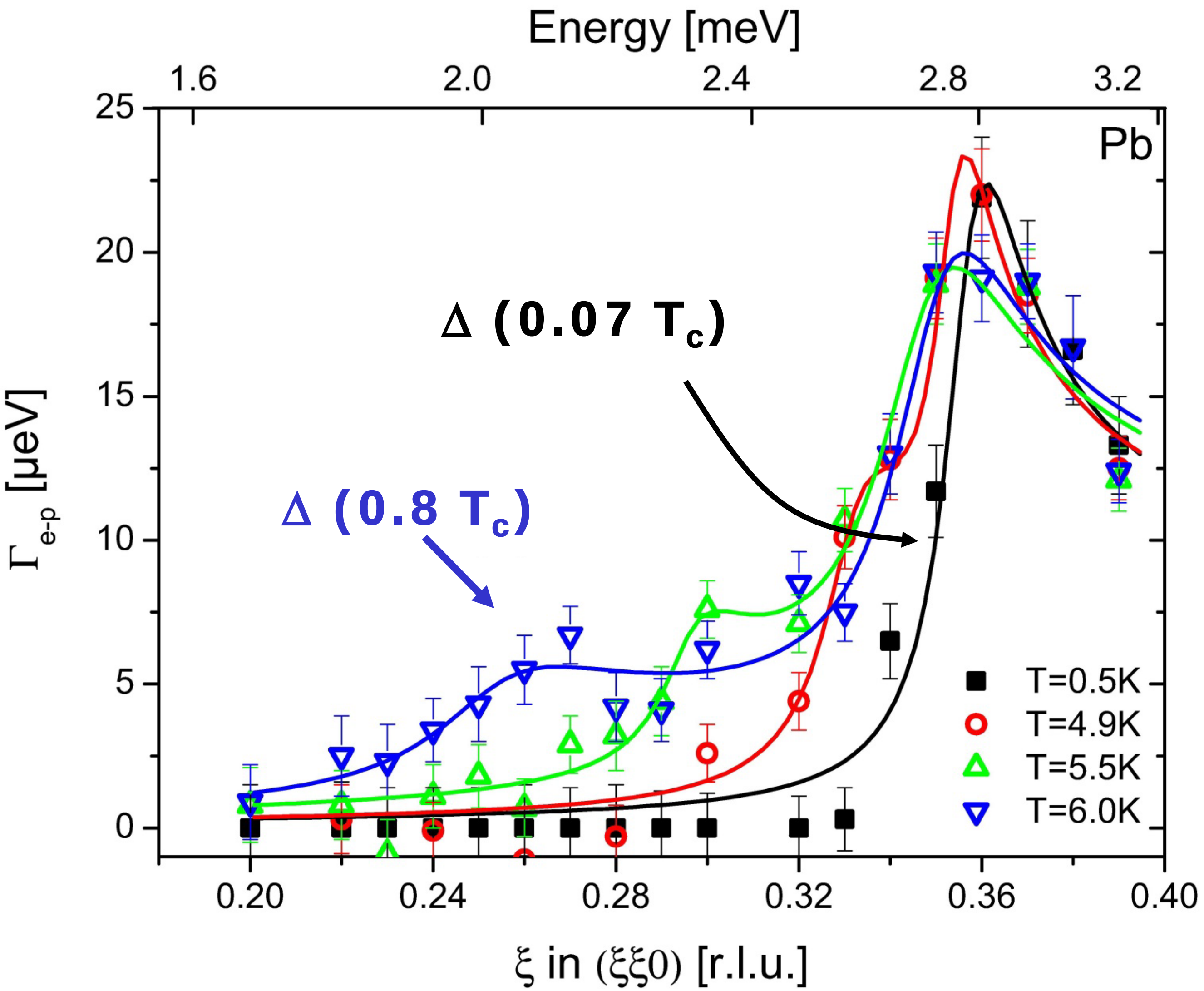

Aynajian et al.
Science 2008

Electron-phonon interaction in Pb

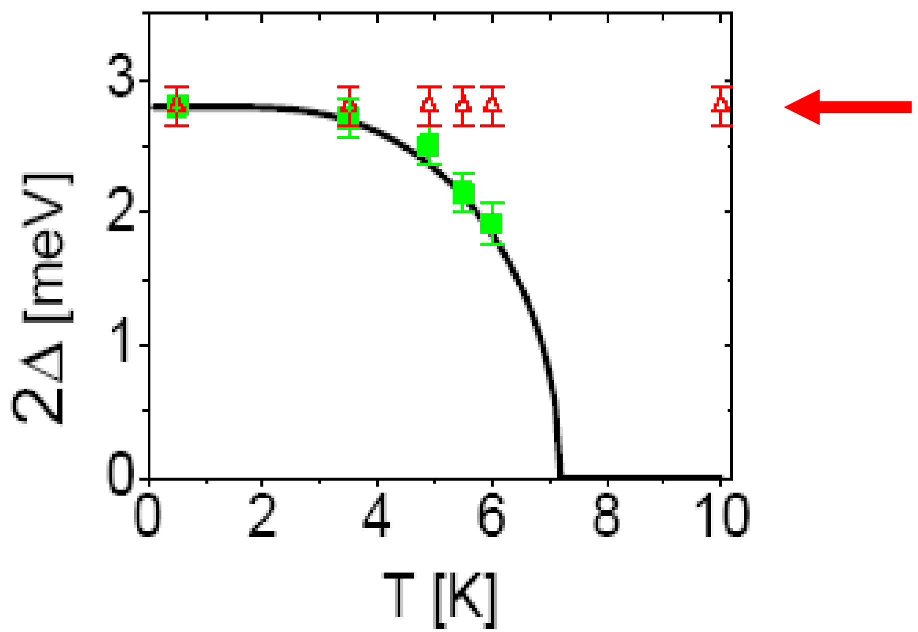

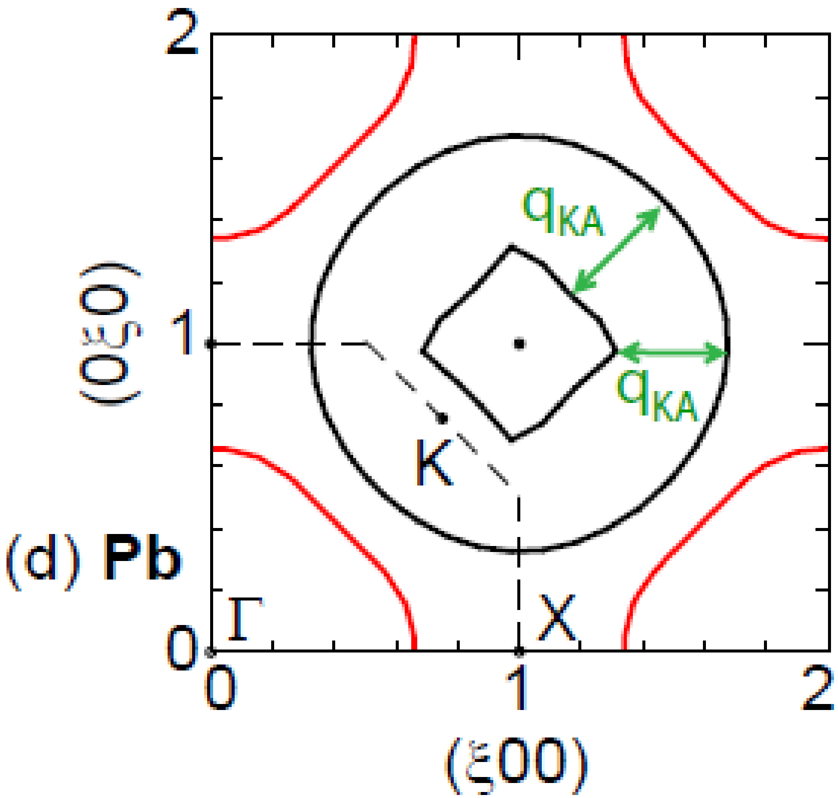

superconducting energy gap

merges with second linewidth

maximum at low T

origin: Kohn anomaly

due to Fermi surface nesting

Accident ?

niobium

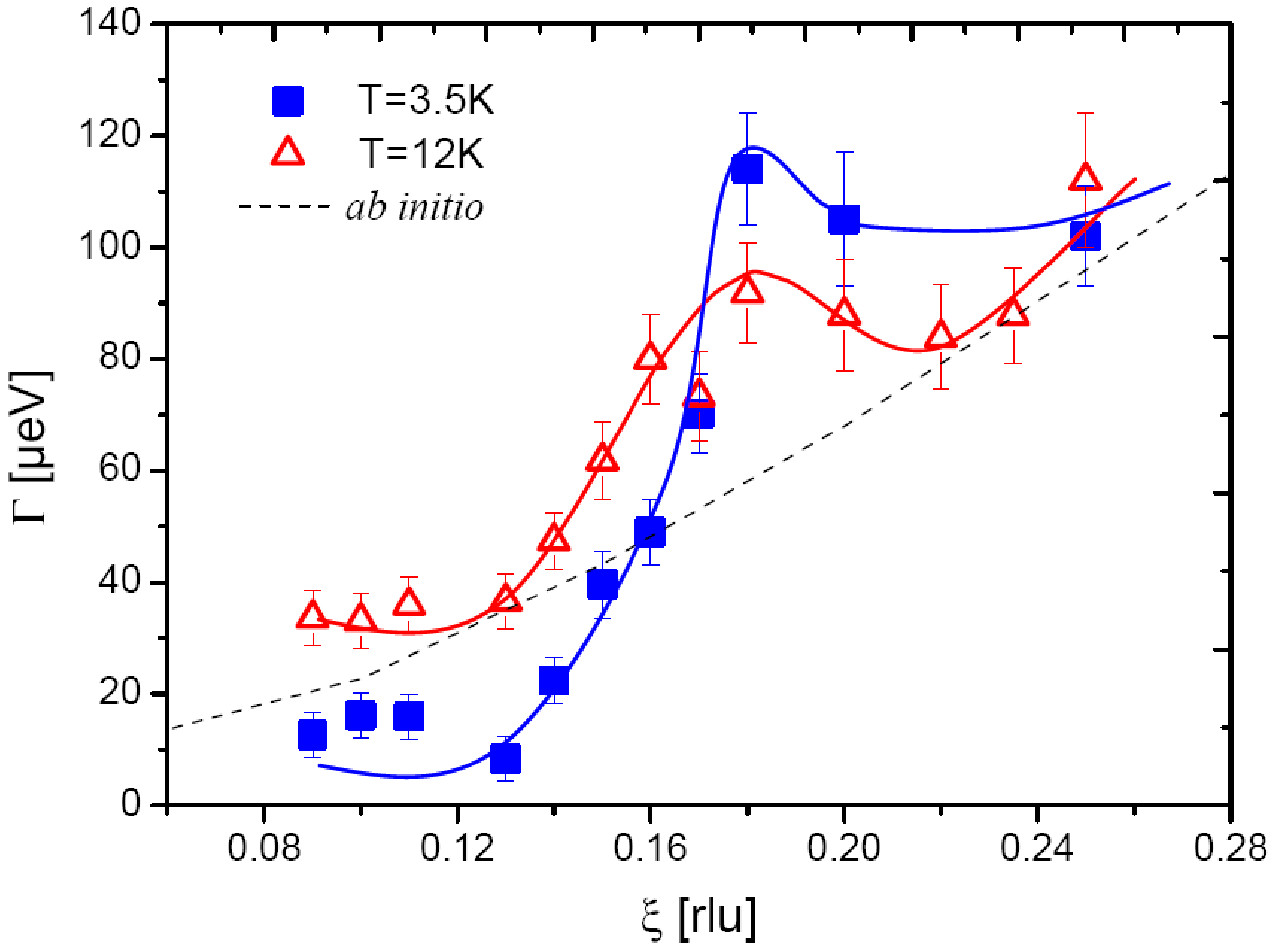

Aynajian et al.
Science 2008

no! same effect observed in Nb

Electron-phonon interaction in Pb

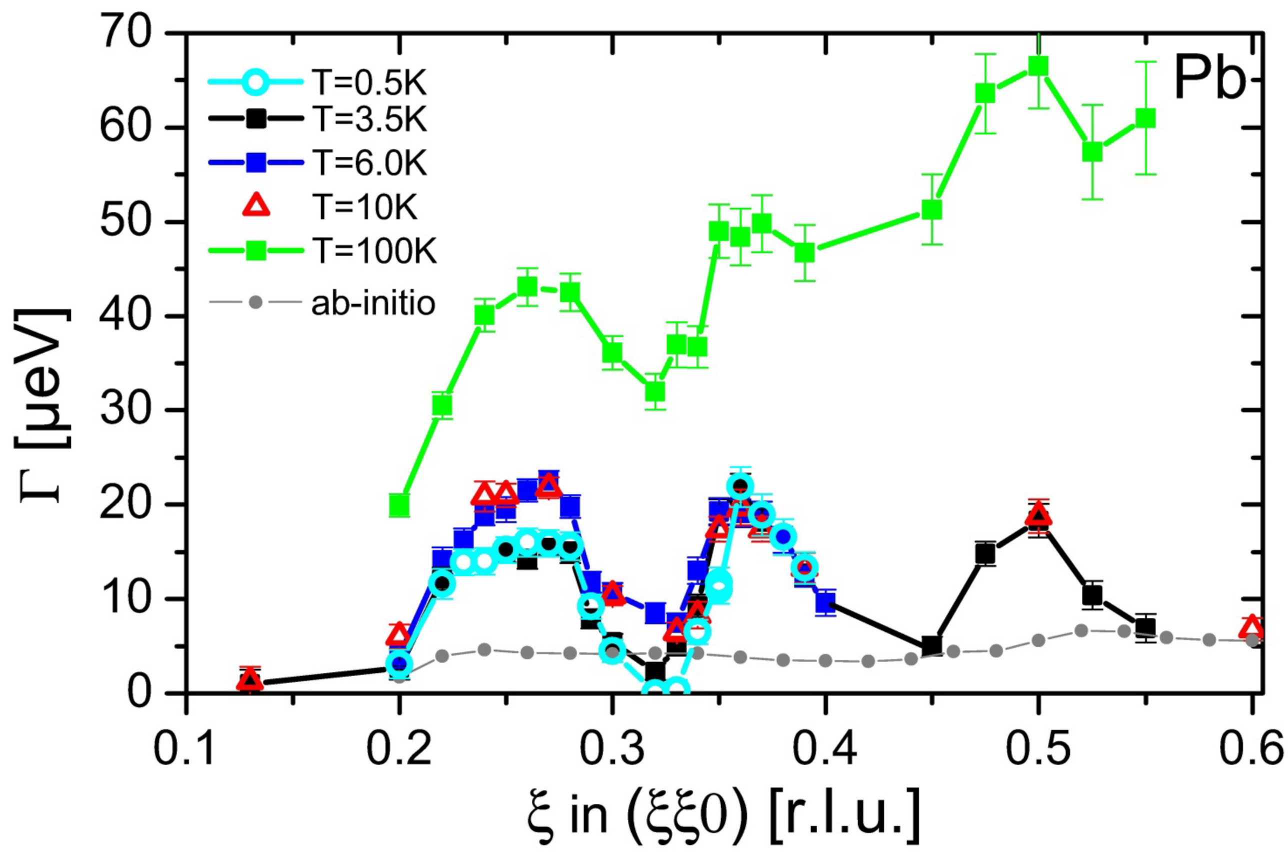

Aynajian et al.
Science 2008

Kohn anomalies not predicted in TA branch by ab-initio LDA calculations

→ many-body correlations beyond LDA

charge density wave fluctations?

für Festkörperforschung

Electron-phonon interaction in Pb and Nb

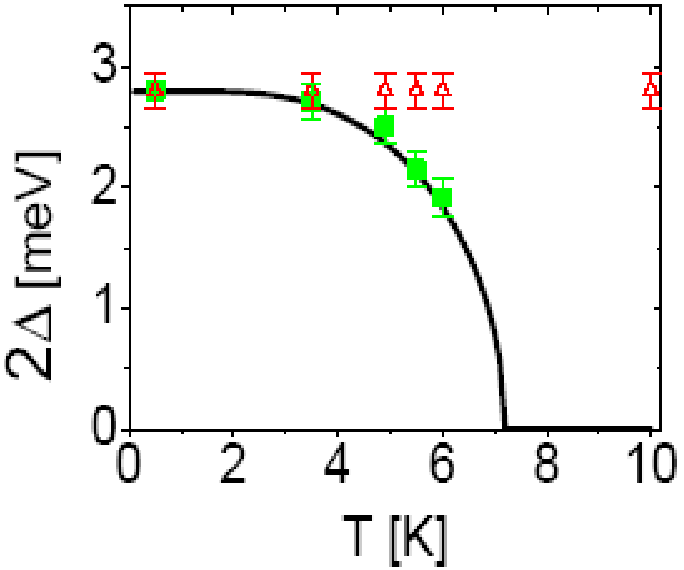

scenario

- many-body effects beyond LDA:
  charge density wave fluctuations
- dynamical nesting $\rightarrow$ Kohn anomalies
- interference between CDW and superconducting fluctuations
  limits growth of superconducting energy gap
- not explain by BCS/Eliashberg theory

Johnston et al., PRB 2011

remains open problem

High temperature superconductivity

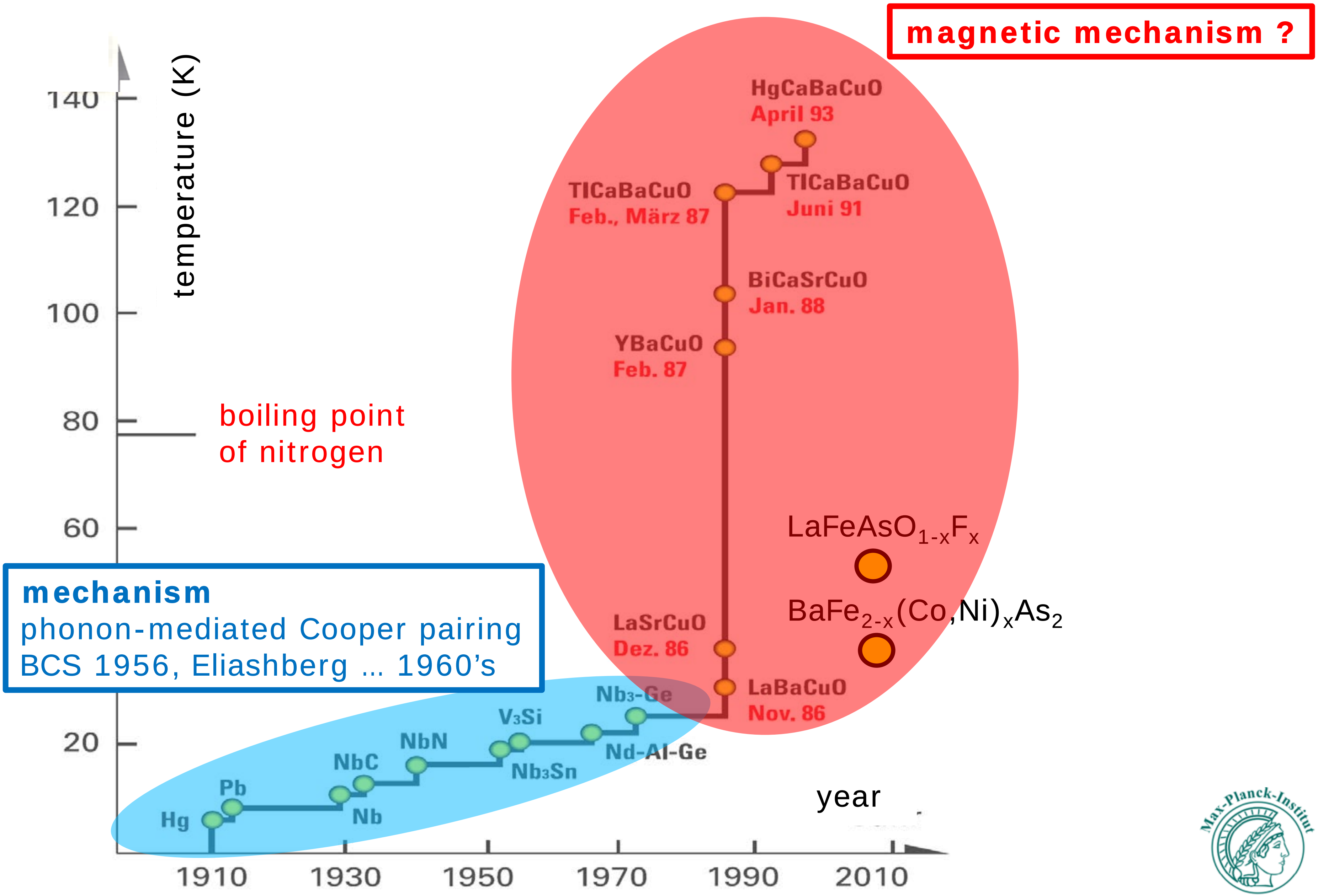

für Festkörperforschung

Copper oxide superconductors

lattice structure

e.g. $YBa_2Cu_3O_{6+x}$ $T_c \leq 93$ K

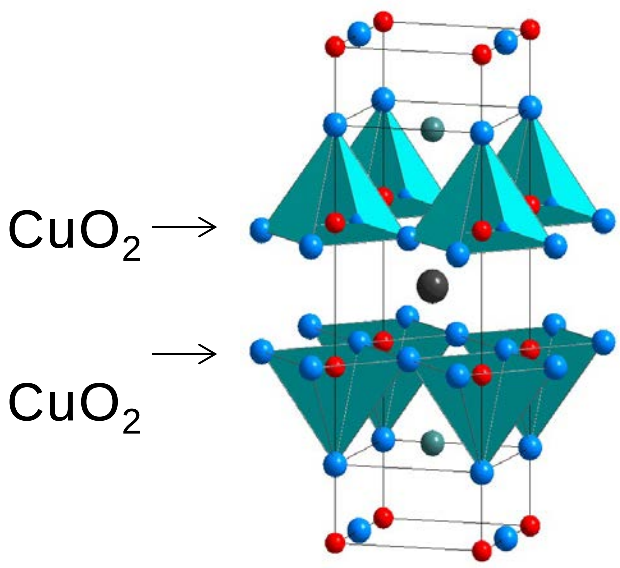

phase diagram

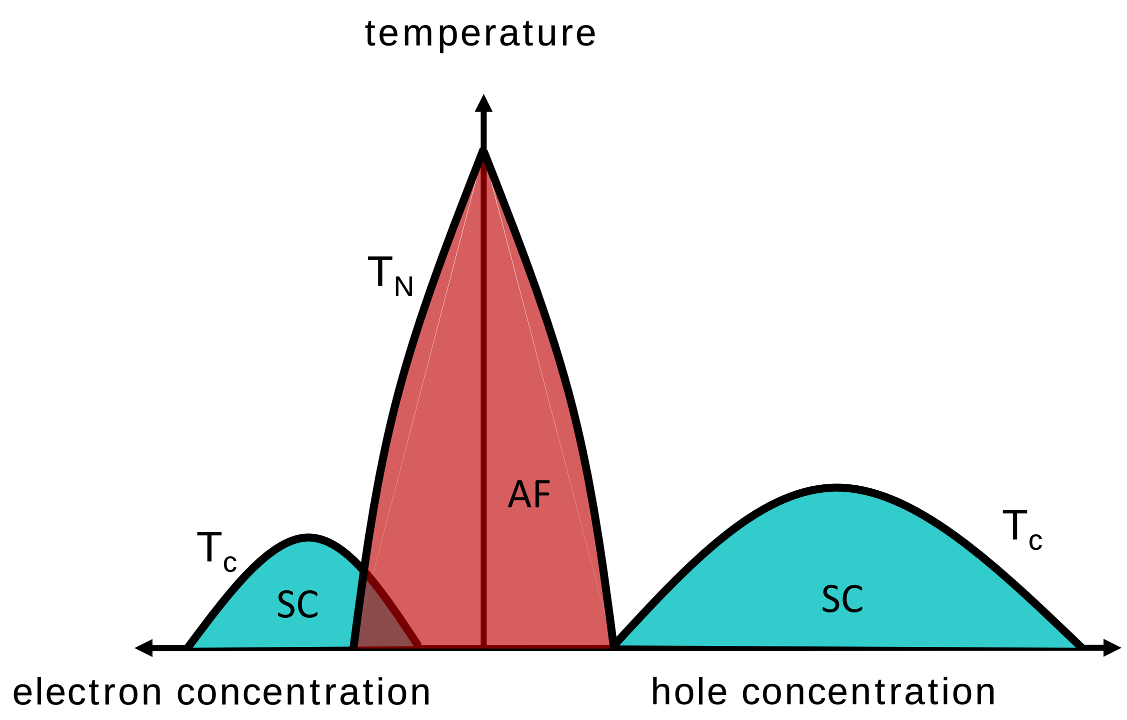

für Festkörperforschung

$YBa_2Cu_3O_{6+x}$

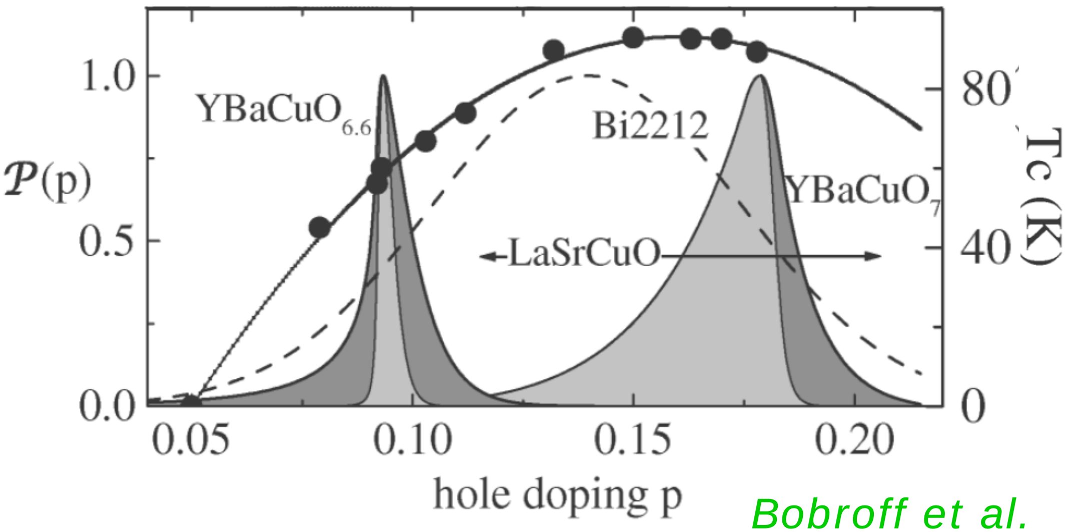

Bobroff et al.
PRL 2002

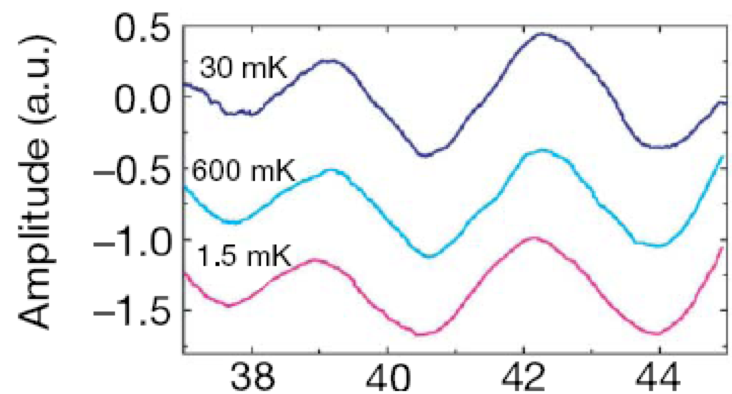

Doiron-Leyraud et al.
Nature 2007

Sebastian et al.
Nature 2008

NMR

→ high homogeneity, low disorder

quantum oscillations

→ fermionic quasiparticles

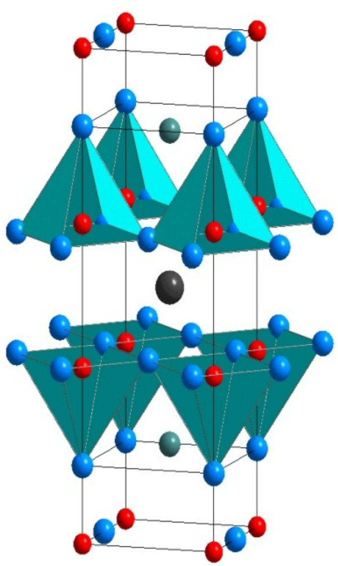

untwinned crystals

scattering & transport probes can discriminate between uniaxial and biaxial modulations

für Festkörperforschung

Iron pnictide superconductors

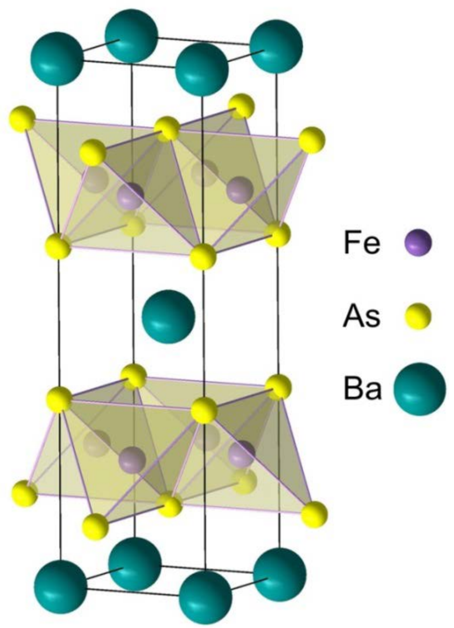

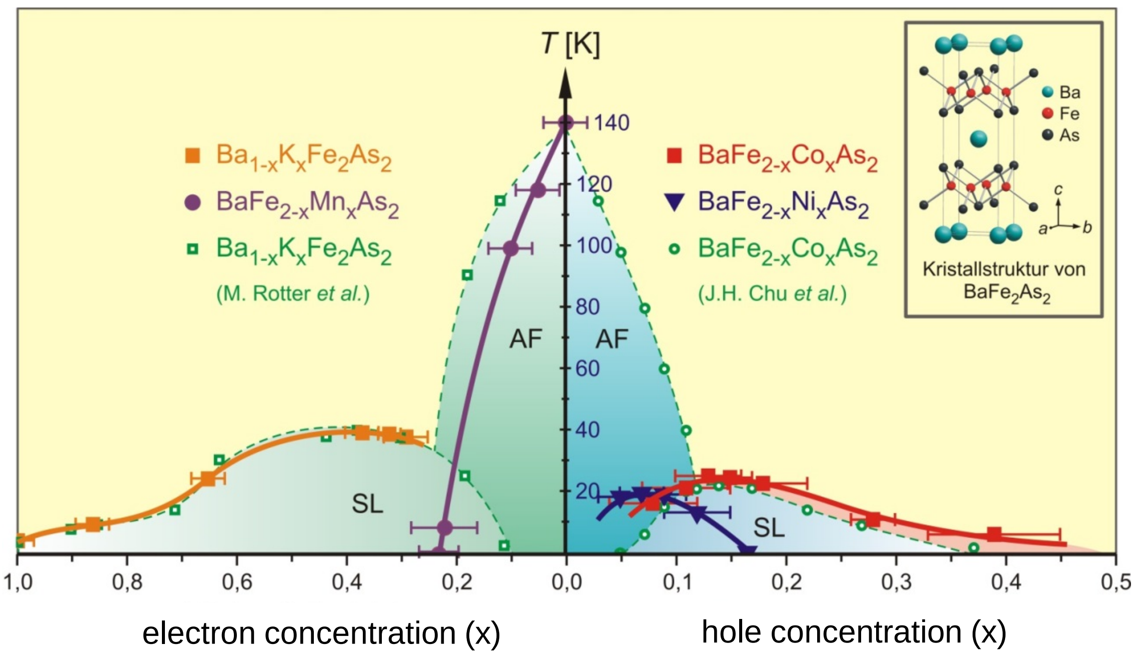

- lattice structure different from cuprates
- phase diagram similar to cuprates
- focus on **magnetic mechanisms** of Cooper pairing

Elastic magnetic neutron scattering

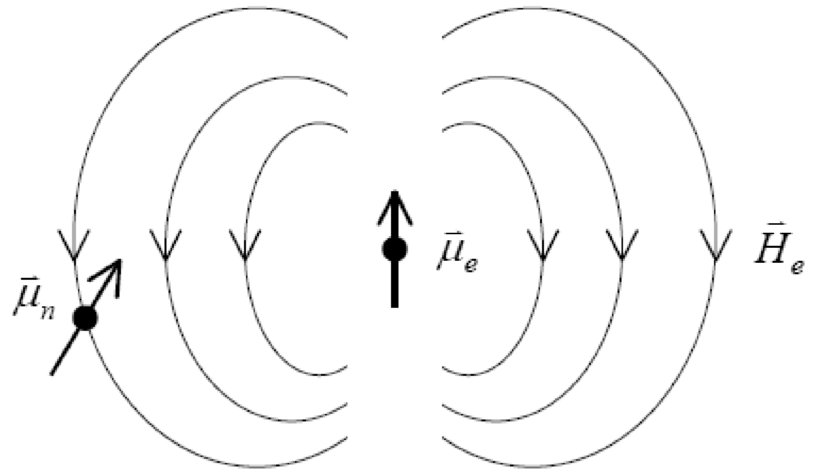

$$\vec{\mu}_e = -2\mu_B \vec{s}_e \text{ with } \mu_B = \frac{e\hbar}{2m_e}$$

$$\vec{\mu}_n = -g_n \mu_N \vec{s}_n \equiv -\gamma \mu_N \vec{\sigma} \text{ with } \mu_N = \frac{e\hbar}{2m_n} \text{ and } \gamma = \frac{g_n}{2} = 1.913$$

$$\frac{d\sigma}{d\Omega} = \left(\frac{m_n}{2\pi\hbar^2}\right)^2 \left|\left\langle \vec{k}_f m_f \middle| H_{\text{int}} \middle| \vec{k}_i m_i \right\rangle\right|^2 \text{ with } H_{\text{int}} = -\vec{\mu}_n \cdot \vec{H}_e$$

Elastic magnetic neutron scattering

$$\vec{A}_e = \frac{\mu_0}{4\pi}\frac{\vec{\mu}_e \times \vec{r}}{|\vec{r}^{\,3}|} = \frac{\mu_0}{4\pi}\vec{\mu}_e \times \vec{\nabla}\frac{1}{|\vec{r}|}$$

$$\vec{H}_e = \vec{\nabla}\times\vec{A}_e = \frac{\mu_0}{4\pi}\vec{\nabla}\times\left(\vec{\mu}_e \times \nabla\frac{1}{|\vec{r}|}\right)$$

collect all prefactors:

$$\left(\frac{m_n}{2\pi\hbar^2}\right)^2 (2\gamma\mu_N\mu_B)^2 \left(\frac{\mu_0}{4\pi}\right)^2 (4\pi)^2 = \boxed{(\gamma r_0)^2}$$

$$\frac{d\sigma}{d\Omega} = \left(\frac{m_n}{2\pi\hbar^2}\right)^2 (2\gamma\mu_N\mu_B)^2 \left|\left\langle \vec{k}_f, m_f \left| \vec{\sigma}_n \cdot \vec{\nabla}\times\left(\vec{s}_e \times \nabla\frac{1}{|\vec{r}|}\right)\right| \vec{k}_i, m_i\right\rangle\right|^2$$

$$\int \frac{d\vec{p}}{|\vec{p}|^2} e^{i\vec{p}\cdot\vec{r}} = 2\pi\int_0^\infty d|\vec{p}| \int_{-1}^{1} e^{i|\vec{p}|\,|\vec{r}|\cos\Theta} d(\cos\Theta) \quad = 2\pi\int_0^\infty d|\vec{p}|\frac{\sin|\vec{p}|\,|\vec{r}|}{|\vec{p}|\,|\vec{r}|} = \frac{2\pi^2}{|\vec{r}|}$$

$\vec{p}$ auxiliary variable

$$\nabla\times\left(\vec{s}_e \times \nabla\frac{1}{|\vec{r}|}\right) = \frac{1}{2\pi^2}\int\frac{d\vec{p}}{|\vec{p}|^2}\,\vec{\nabla}\times\left(\vec{s}_e\times\vec{\nabla}\right) e^{i\vec{p}\cdot\vec{r}}$$

$$= \frac{1}{2\pi^2}\int \hat{p}\times\left(\vec{s}_e\times\hat{p}\right) e^{i\vec{p}\cdot\vec{r}} d\vec{p}$$

$$\left\langle \vec{k}_f \left| \nabla\times\left(s_e\times\nabla\frac{1}{|\vec{r}|}\right)\right| \vec{k}_i\right\rangle = \frac{1}{2\pi^2}\int d\vec{r}\,e^{-i\vec{Q}\cdot\vec{r}}\int d\vec{p}\;\hat{p}\times\left(\vec{s}_e\times\hat{p}\right) e^{i\vec{p}\cdot\vec{r}}$$

$$\boxed{= 4\pi\,\underbrace{\hat{Q}\times\left(\vec{s}_e\times\hat{Q}\right)}_{\equiv\vec{s}_{e\perp}}}$$

Elastic magnetic neutron scattering

one electron

$$\frac{d\sigma}{d\Omega}=(\gamma r_0)^2\left|\langle m_f|\vec{\sigma}\cdot\vec{s}_{e\perp}|m_i\rangle\right|^2 \qquad r_0\ (=2.8\times10^{-5}\,\mathring{A}$$

"classical electron radius"

$$\langle m_f|\vec{\sigma}\cdot\vec{s}_{e\perp}|m_i\rangle = s_{e\perp}\langle m_f|\sigma_z|m_i\rangle = \begin{cases} s_{e\perp} & \text{if } m_f=m_i \\ 0 & \text{otherwise}\end{cases}$$

non-spin-flip

$$\sigma_z \rightarrow \sigma_x,\ \sigma_y$$

spin-flip (not possible for nuclear scattering)

average for unpolarized beam

$$\frac{d\sigma}{d\Omega}=(\gamma r_0)^2\left|\vec{s}_{e\perp}\right|^2 \qquad \vec{s}_{e\perp}=4\pi\,\hat{Q}\times\left(\vec{s}_e\times\hat{Q}\right)$$

projection of the electron spin perpendicular to $\vec{Q}$

separate nuclear and magnetic neutron scattering by **spin polarization analysis**

Max-Planck-Institut für Festkörperforschung

Elastic magnetic neutron scattering

one atom

approximated as magnetized sphere, magnetization density *M(r)*

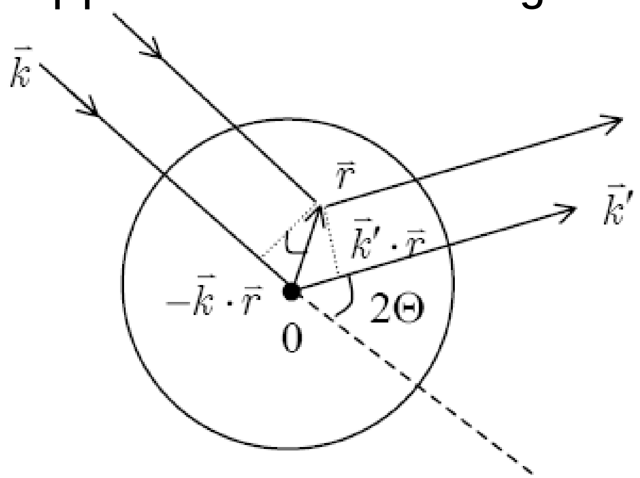

elastic scattering: $|\vec{k}| = |\vec{k}'|$

$|\vec{r}| \ll |\vec{R}|$

phase difference between wave scattered at 0 and at $\vec{r}$: $(\vec{k} - \vec{k}') \cdot \vec{r} \equiv \vec{Q} \cdot r$

$$\frac{d\sigma}{d\Omega} = (\gamma r_0)^2 \left[1 - (\hat{\eta} \cdot \hat{Q})^2\right] \left|f(\vec{Q})\right|^2$$

$$f(\vec{Q}) = \frac{1}{2\mu_B} \int \mathcal{M}(\vec{r})\, e^{-i\vec{Q}\cdot\vec{r}}$$ magnetic form factor

$$\vec{\mathcal{M}}(\vec{r}) = \mathcal{M}(\vec{r})\, \hat{\eta}$$ magnetic dipole moment density

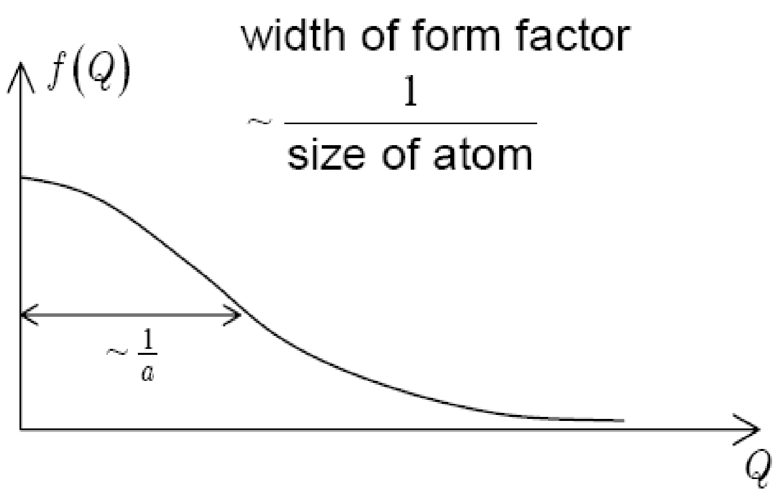

Elastic magnetic neutron scattering

generalization for collinear magnets

$$\frac{d\sigma}{d\Omega} = (\gamma r_0)^2 \left[1-\left(\hat{\eta}\cdot\hat{Q}\right)^2\right] \left|\sum_{\vec{R}} (\pm) f_{\vec{R}}\left(\vec{Q}\right) e^{i\vec{Q}\cdot\vec{R}}\right|^2$$

Bragg peaks

$$= (\gamma r_0)^2 \left[1-\left(\hat{\eta}\cdot\hat{Q}\right)^2\right] N \frac{(2\pi)^3}{V_0} \sum_{\vec{K}_M} \left|F_M\left(\vec{K}_M\right)\right|^2 \delta\left(\vec{Q}-\vec{K}_M\right)$$

polarization factor

$$F_M\left(\vec{Q}\right) = \sum_{\vec{d}} (\pm) f_{\vec{d}}\left(\vec{Q}\right) e^{i\vec{Q}\cdot\vec{d}}$$

magnetic structure factor

$\vec{K}_M$ magnetic reciprocal lattice vectors

Example one-dimensional ferromagnet

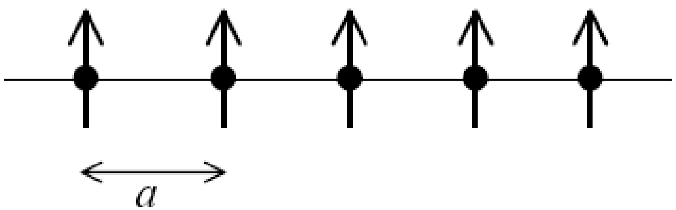

nuclear and magnetic unit cells identical $\Rightarrow K_M = K_N = \frac{2\pi}{a} n, \quad n$ integer.

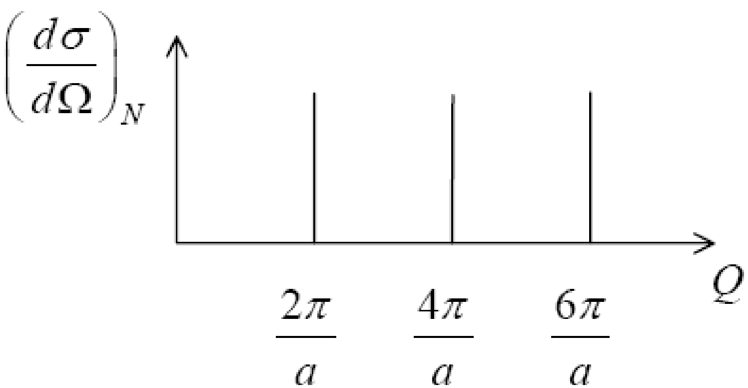

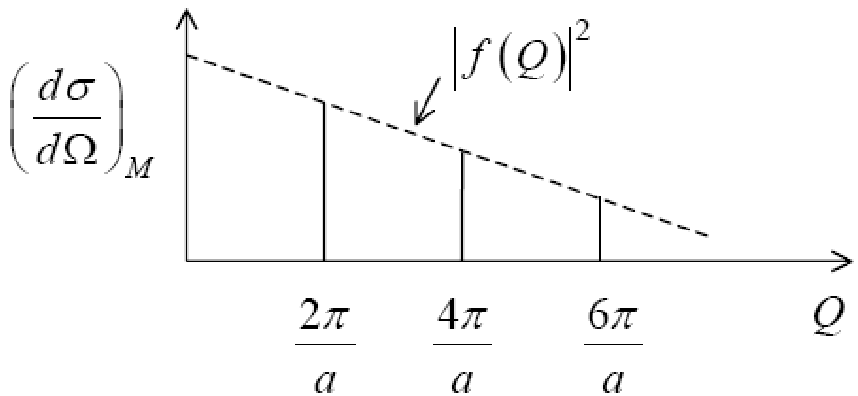

use **interference** between nuclear and magnetic scattering
to create spin-polarized neutrons

$$\frac{d\sigma}{d\Omega} \sim |b|^2 + |\hat{\eta}|^2 + b\hat{\eta}$$

(up to prefactors)

Example one-dimensional antiferromagnet

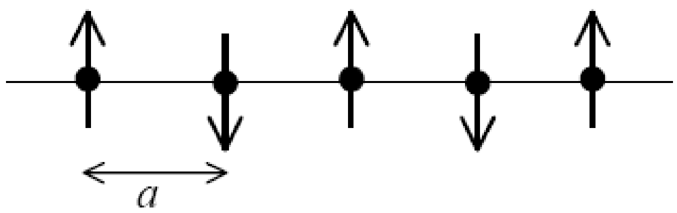

magnetic unit cell twice as large as nuclear unit cell $\Rightarrow\ K_M = \frac{\pi}{a} n \neq K_N = \frac{2\pi}{a} n$

$$|F_M|^2 = |f(Q)|^2 \; \left|+1 - e^{iQa}\right|^2 = 4|f(Q)|^2 \sin^2\frac{Qa}{2} = \begin{cases} 4|f(Q)|^2 & \text{for } n \text{ odd} \\ 0 & \text{for } n \text{ even} \end{cases}$$

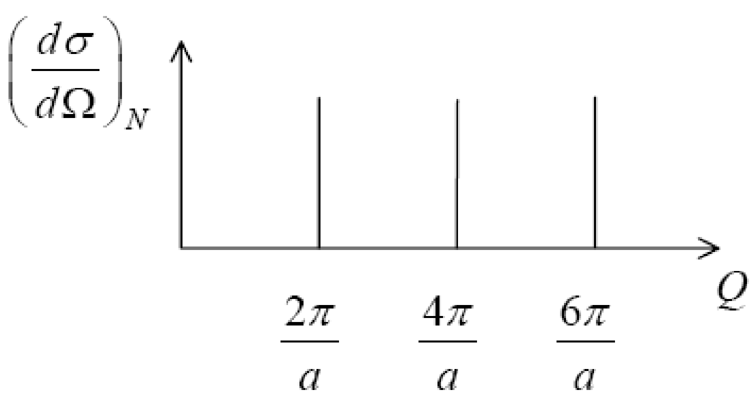

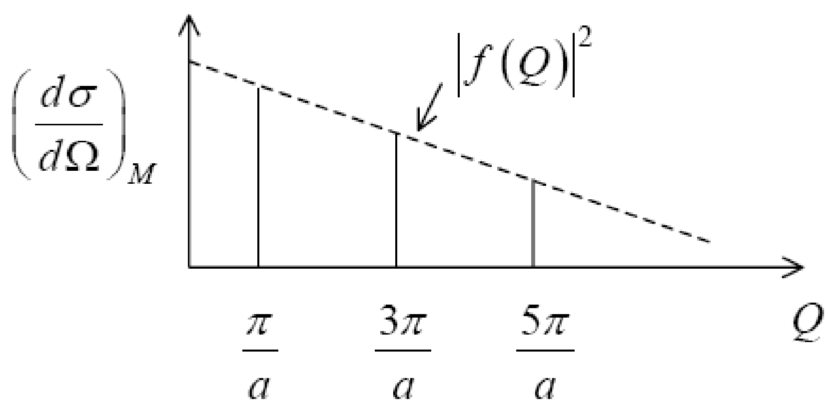

Neutron diffractometers

powder

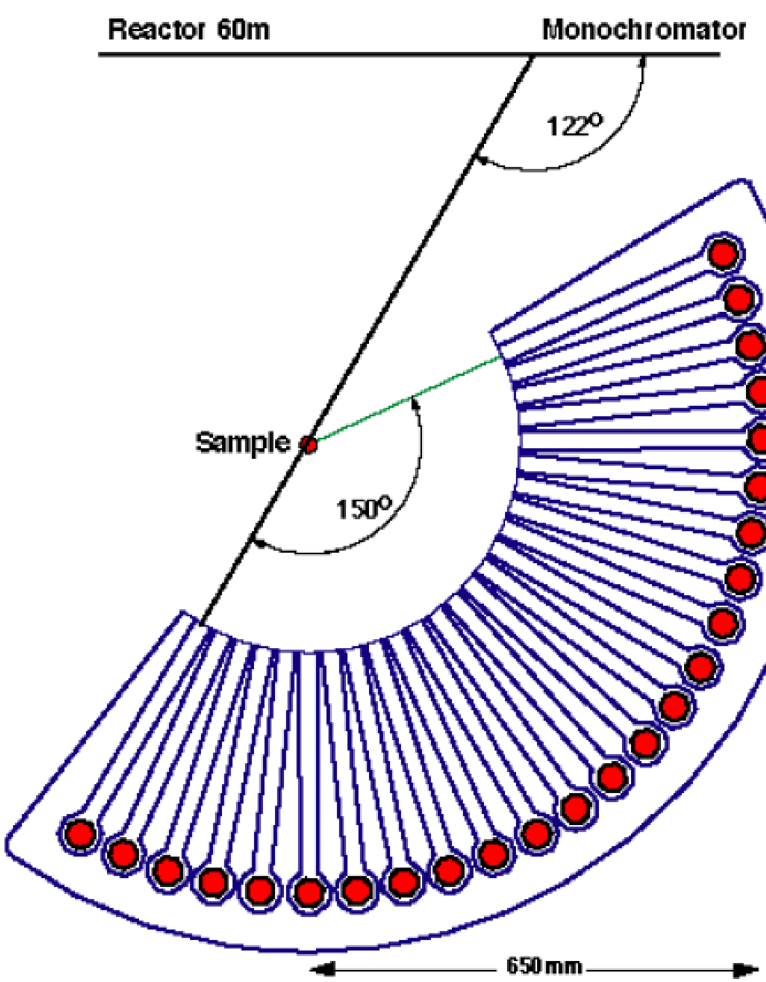

single crystal

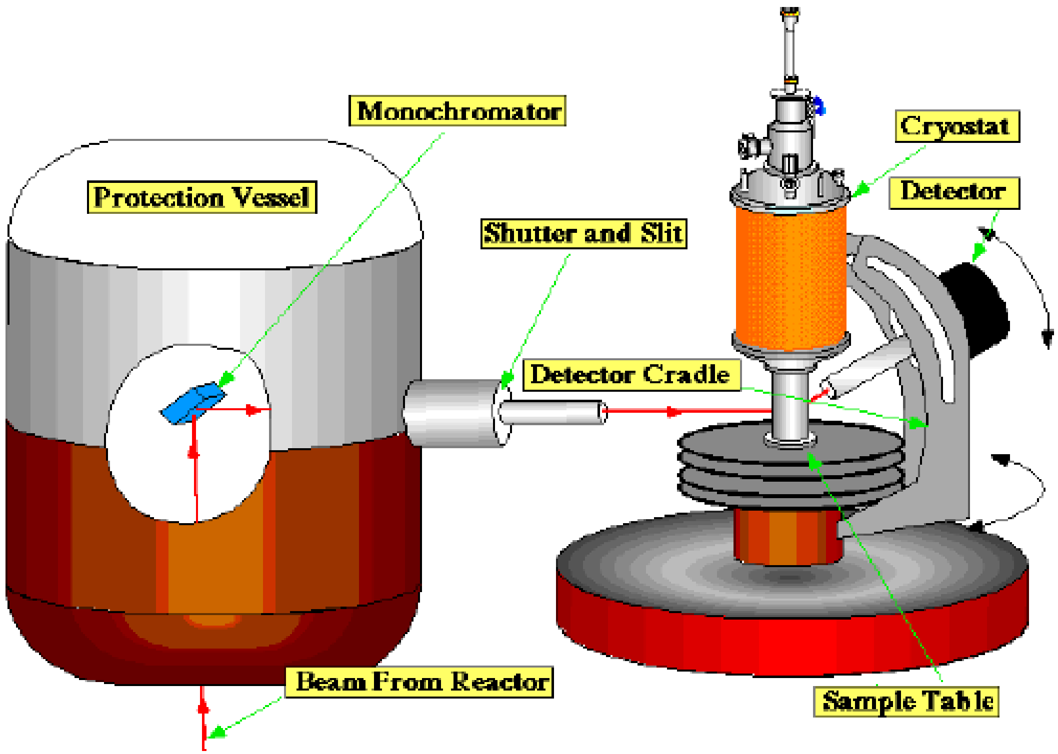

für Festkörperforschung

$YBa_2Cu_3O_6$ spin structure

spin orientation extracted from magnetic Bragg reflections

Tranquada et al., PRB 1989

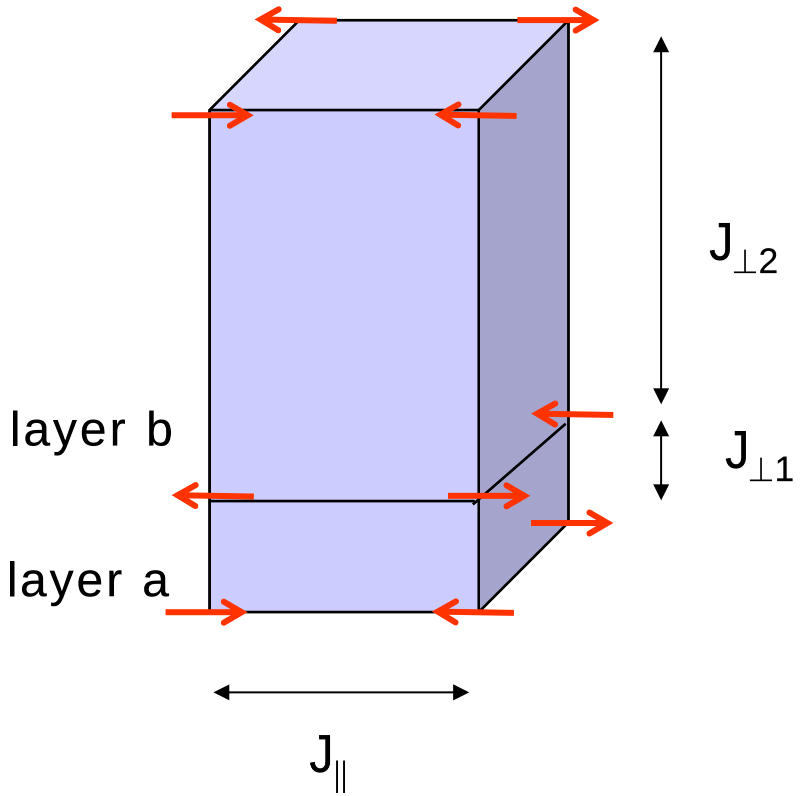

$$H = \Sigma_{ij} (J_{||} S_i^{(a,b)} \bullet S_j^{(a,b)}) + \Sigma_i (J_{\perp 1} S_i^{(a)} \bullet S_i^{(b)} + J_{\perp 2} S_i^{(b)} \bullet S_i^{(a)})$$

Sign, but not strength of exchange parameters determined by elastic neutron scattering

Phase diagram of $YBa_2Cu_3O_{6+x}$

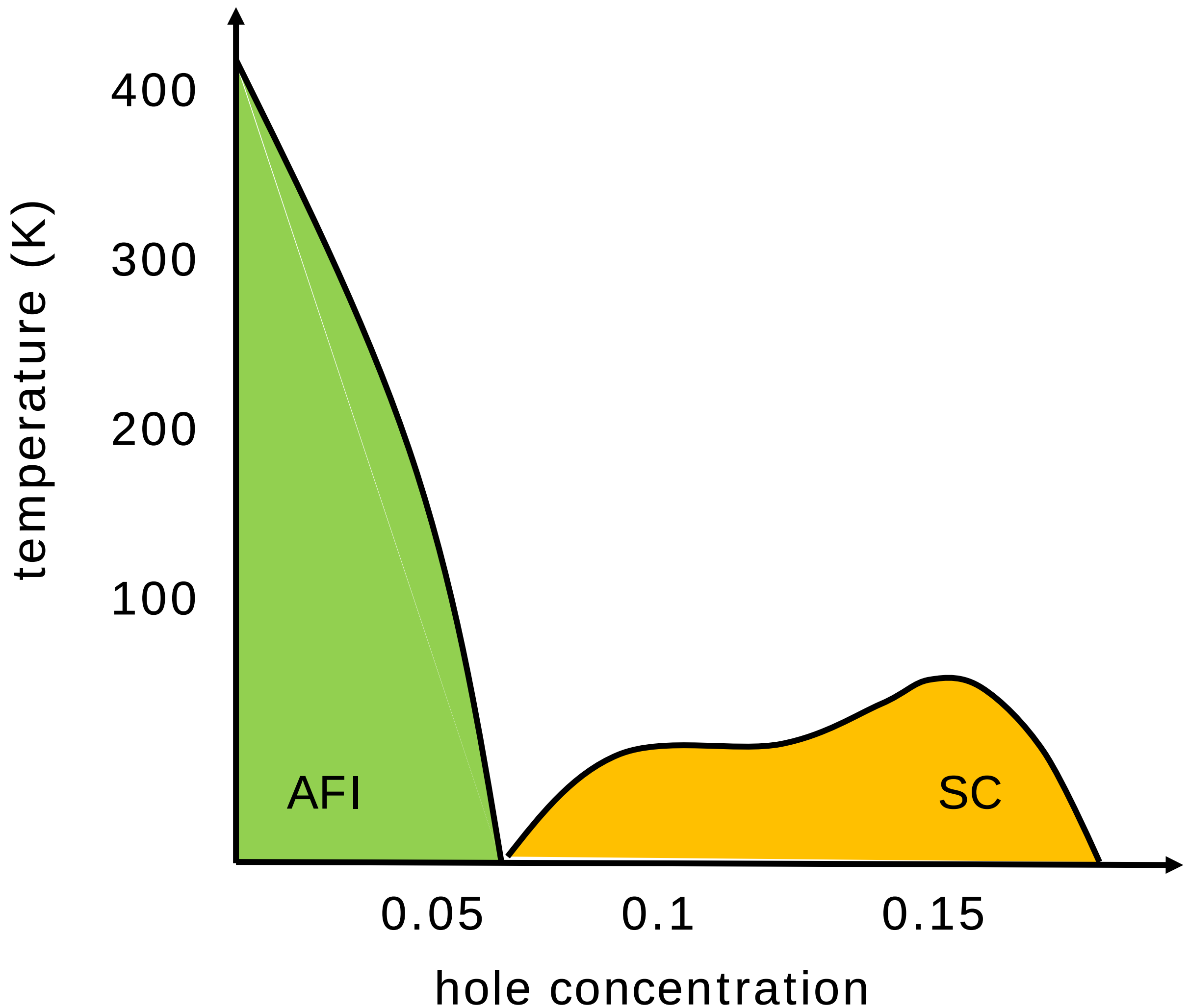

Spin-polarized neutrons

neutron spin operator

$$\left(\frac{d\sigma}{d\Omega}\right)_M = (\gamma r_0)^2 \left|\langle m_f | \vec{\sigma}\cdot\hat{\eta}_\perp | m_i \rangle\right|^2 \sum_{\vec{K}_M} \left|F_M(\vec{Q})\right|^2 \delta\left(\vec{Q}-\vec{K}_M\right)$$

neutron spin states
defined by spin polarizers

manipulate relative orientation of vectors σ, η, Q

→ accurate determination of complex spin structures

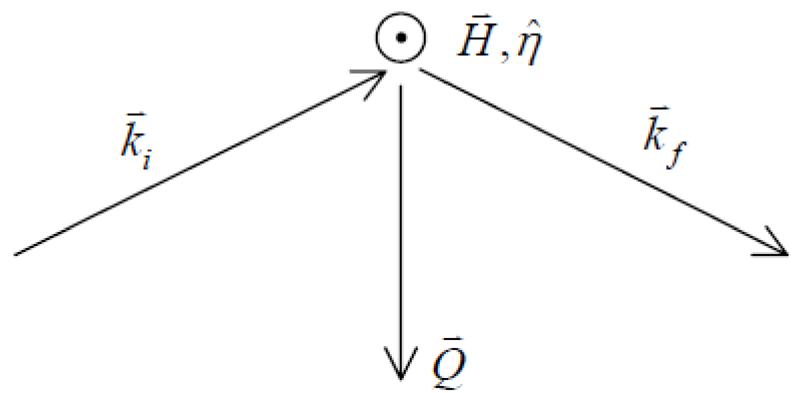

Spin-polarized neutrons

Polarized neutron spectrometer

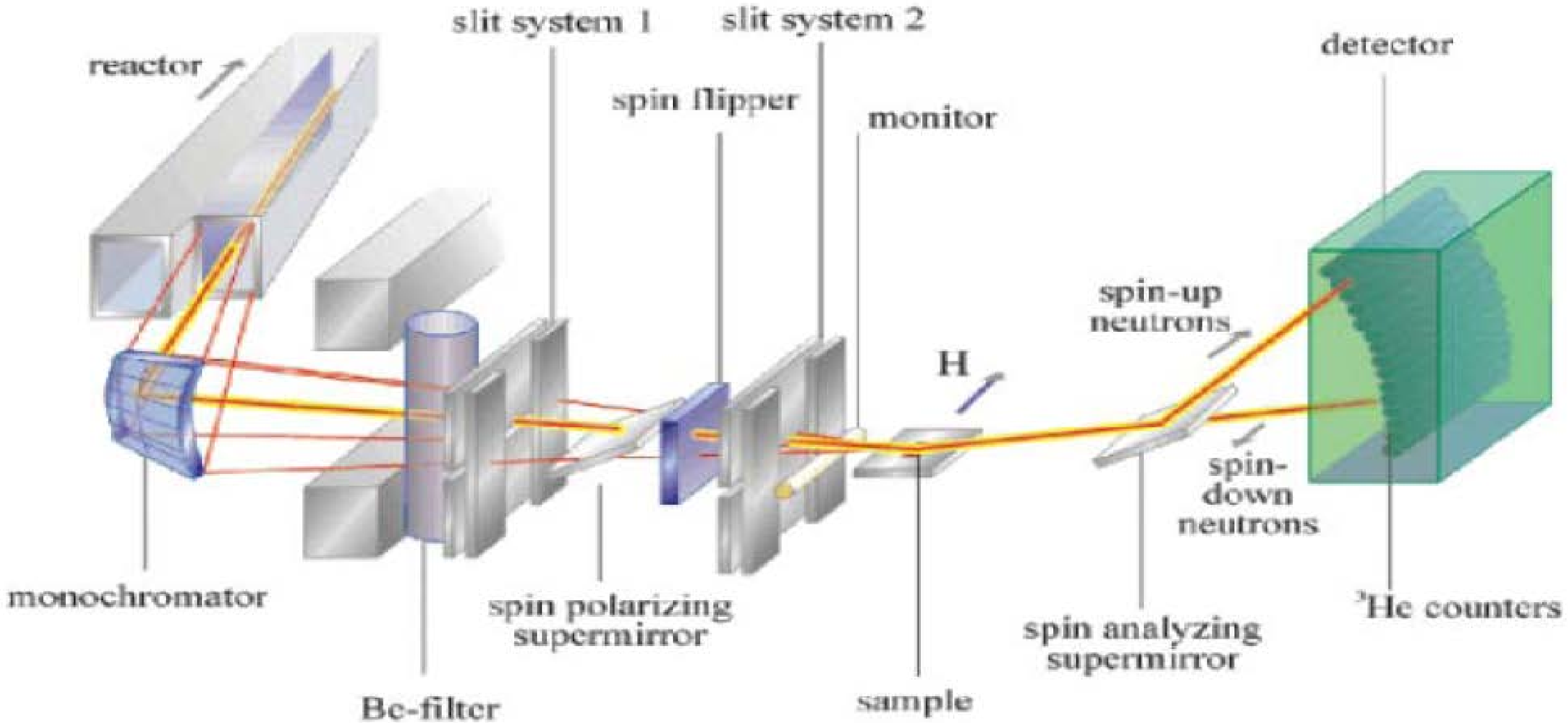

Spin density wave

spin structures from spin-polarized neutron scattering

undoped $YBa_2Cu_3O_6$

commensurate antiferromagnetism

lightly doped $YBa_2Cu_3O_{6+x}$

noncollinear incommensurate structure,

facilitates propagation of doped holes

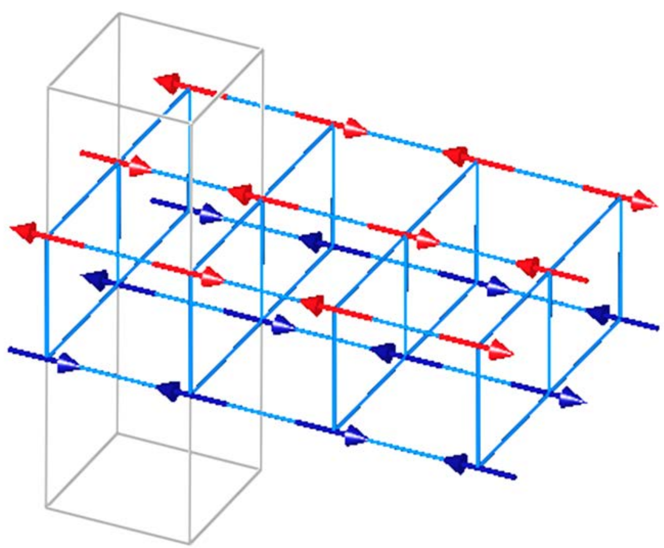

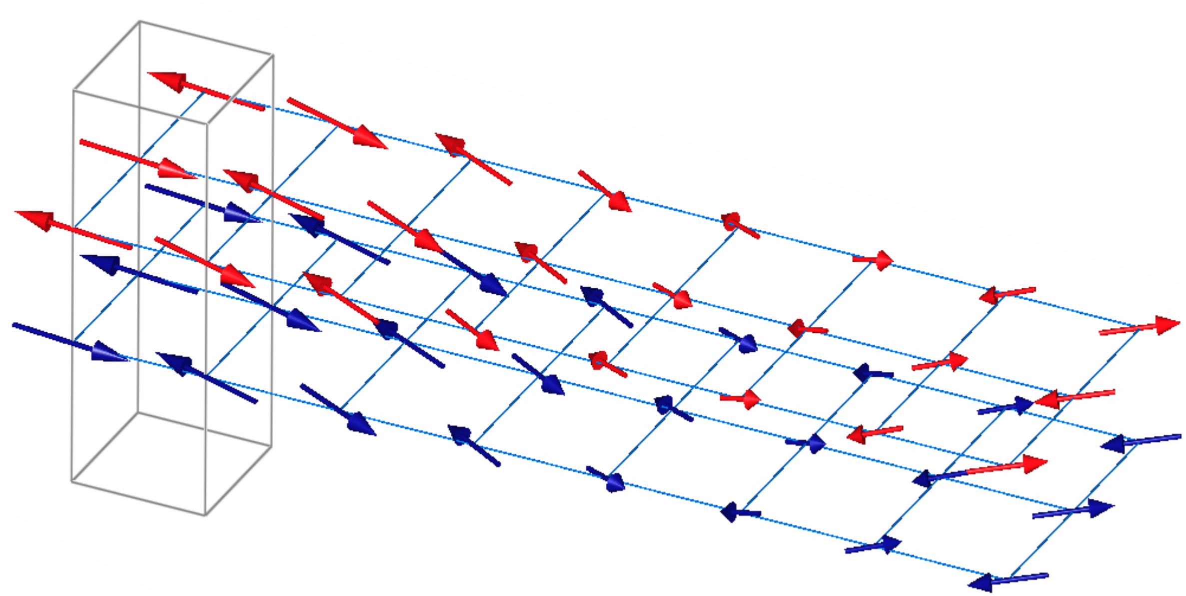

Haug et al., PRL 2009, NJP 2012
Porras, Loew et al.

Max-Planck-Institut für Festkörperforschung

Competing order in $YBa_2Cu_3O_{6+x}$

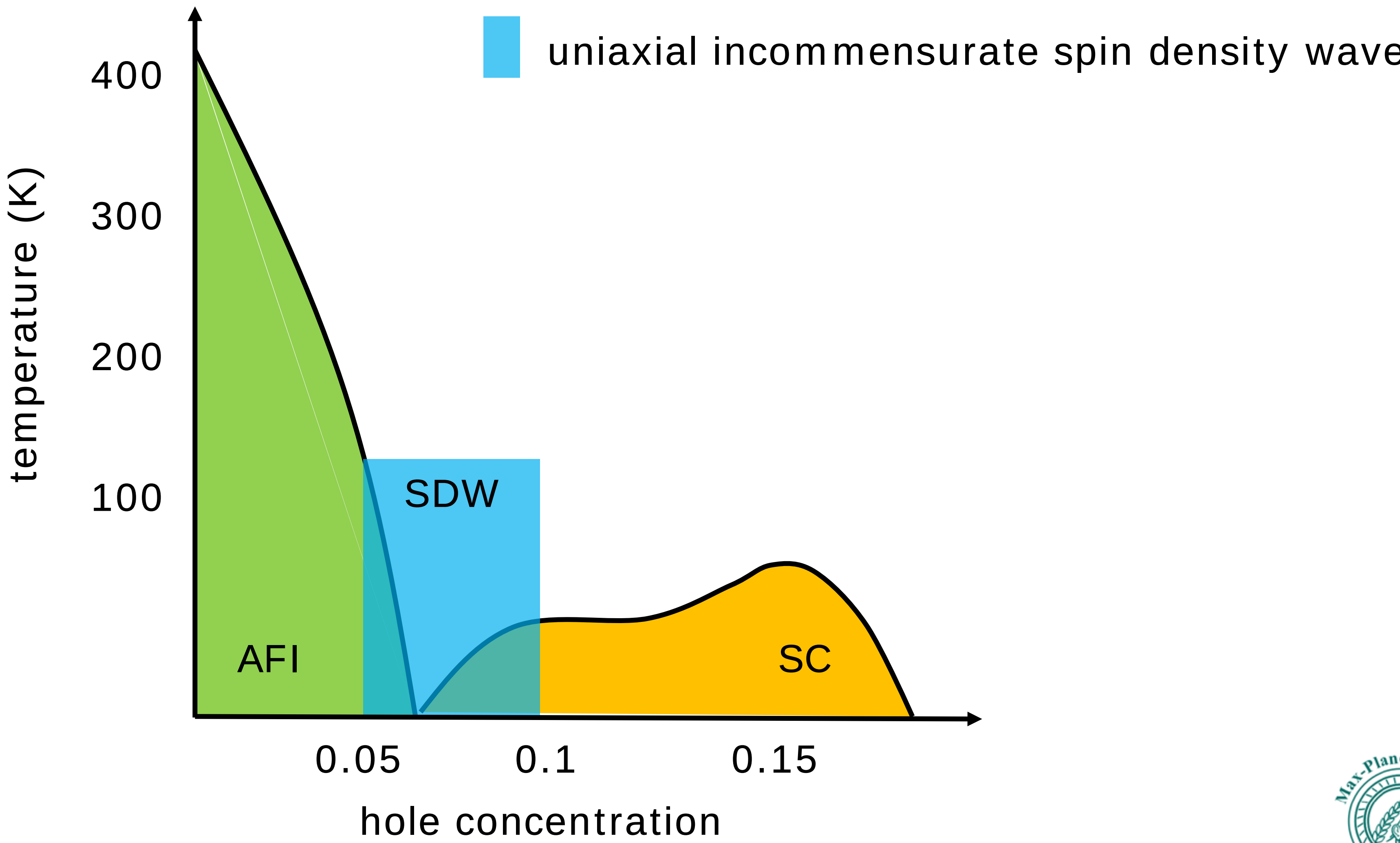

Inelastic magnetic neutron scattering

polarization factor

$$\frac{d^2\sigma}{d\Omega\, dE} = (\gamma r_0)^2 \frac{k_f}{k_i} N \left| F(\mathbf{Q}) \right|^2 e^{-2W} \sum_{\alpha\beta} (\delta_{\alpha\beta} - \hat{Q}_\alpha \hat{Q}_\beta) S^{\alpha\beta}(\mathbf{Q}, \omega)$$

$$S^{\alpha\beta}(\mathbf{Q}, \omega) = \frac{1}{2\pi\hbar} \int \sum_l e^{i\mathbf{Q}\mathbf{r}_l} \left\langle S_0^\alpha(0) S_l^\beta(t) \right\rangle e^{-i\omega t} dt$$

spin-spin correlation function

fluctuation-dissipation theorem

$$S^{\alpha\beta}(\mathbf{Q}, \omega) = \frac{1}{\pi (g\mu_{\mathrm{B}})^2} \frac{1}{1 - e^{-\hbar\omega\beta}} \chi''_{\alpha\beta}(\mathbf{Q}, \omega)$$

$$\chi''(\mathbf{Q}, \omega) = \mathrm{Tr}\left[\chi''_{\alpha\beta}(\mathbf{Q}, \omega)\right]/3$$

dynamical magnetic susceptibility
response to time- and position-dependent H-field

$$\frac{d^2\sigma}{d\Omega\, dE} = 2(\gamma r_0)^2 \frac{k_f}{k_i} N \left| F(\mathbf{Q}) \right|^2 e^{-2W} \frac{1}{\pi (g\mu_{\mathrm{B}})^2} \frac{1}{1 - e^{-\hbar\omega\beta}} \chi''(\mathbf{Q}, \omega)$$

Inelastic magnetic neutron scattering

localized electrons → Heisenberg antiferromagnet, magnon creation

$$\frac{d^2\sigma}{d\Omega\, dE} = (\gamma r_0)^2 \frac{k_f}{k_i} |F(\mathbf{Q})|^2 e^{-2W} \frac{(2\pi)^3}{4Nv_0} \{1 - (\hat{Q}\hat{\eta})^2\} \times$$

$$\sum_{a=0,1} \sum_{q, K_m} \langle n_{q,a} + 1 \rangle \, \delta(\omega_{q,a} - \omega) \, \delta(\mathbf{Q} - \mathbf{q} - \mathbf{K_m})$$

magnon dispersions

für Festkörperforschung

$YBa_2Cu_3O_6$ magnons

$$H = \Sigma_{ij} \left(J_{\parallel}\, S_i^{(a,b)} \bullet S_j^{(a,b)}\right) + \Sigma_i \left(J_{\perp 1}\, S_i^{(a)} \bullet S_i^{(b)} + J_{\perp 2}\, S_i^{(b)} \bullet S_i^{(a)}\right)$$

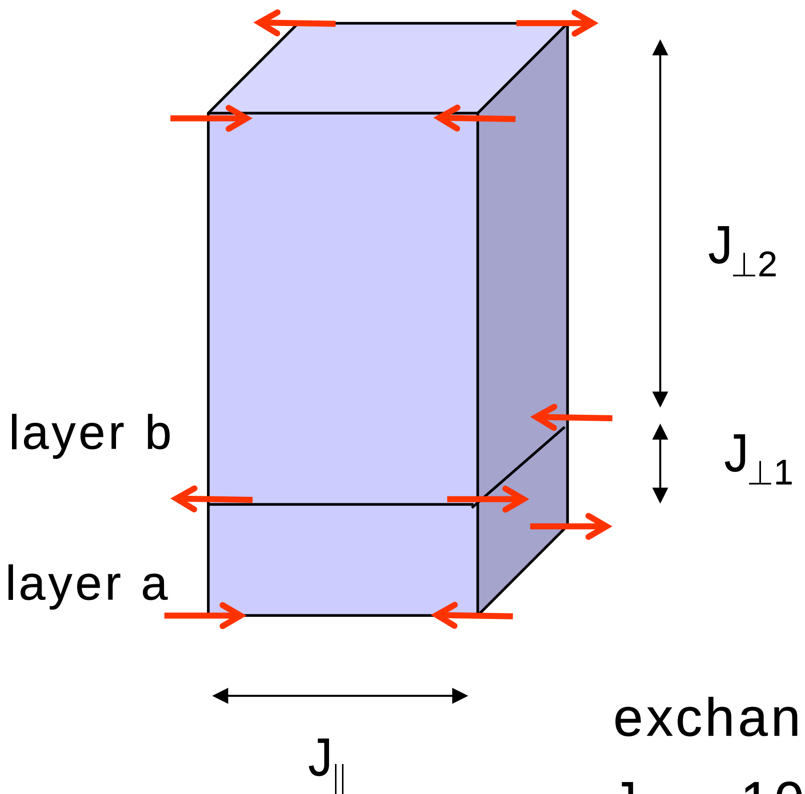

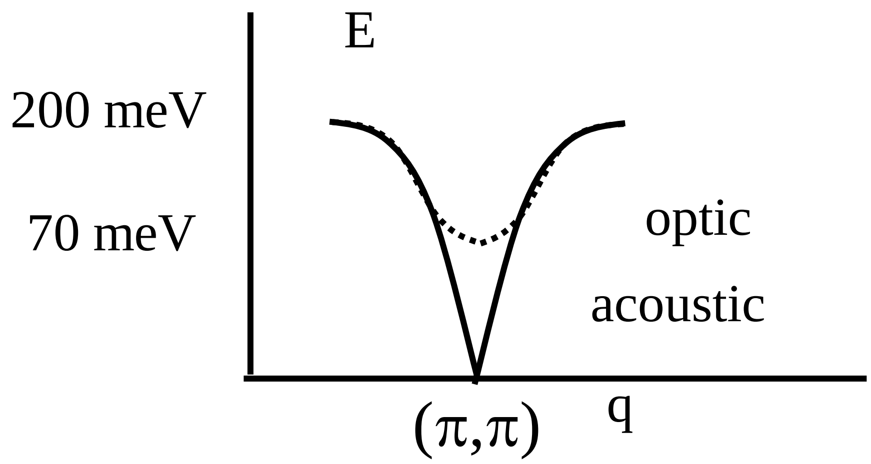

exchange parameters from magnon dispersions

$J_{\parallel}$ ~ 100 meV

$J_{\perp 1}$ ~ 10 meV

$J_{\perp 2}$ ~ 0.01 meV

Tranquada et al., PRB 1989
Reznik et al., PRB 1996

Max-Planck-Institut für Festkörperforschung